RSC Advances

REVIEW

View Article Online
View Journal | View Issue

Cite this: *RSC Adv.*, 2026, **16**, 758

Magnetized phyto-adsorbents for industrial dye removal: functionalization and mechanistic insights for sustainable wastewater remediation

Shaikh Aliya Aijaz,[a] Zaryab Shafi and[b] and Mohammad Shahid *[c]

Industrial effluents from textile, leather, and dye manufacturing are major sources of water pollution, often containing synthetic dyes such as azo, reactive, and basic classes. These dyes are highly stable, toxic, and persistent, posing significant risks to both the ecosystem and human health. Conventional treatment methods, such as coagulation, oxidation, and activated carbon filtration, are often costly and operationally challenging, highlighting the need for sustainable alternatives. This review provides a comprehensive analysis of magnetized plant-based adsorbents, focusing on their composition, synthesis strategies, adsorption behaviour, and real-world potential. Incorporating Fe_3O_4 nanoparticles (NPs) into lignocellulosic biomass through co-precipitation, sol–gel, hydrothermal, or *in situ* embedding techniques enhances surface functionality, adsorption kinetics, and recovery efficiency. Adsorption mechanisms, modeled using Langmuir and Freundlich isotherms and pseudo-second-order kinetics, demonstrated the capacities of common dyes. Comparative studies show that magnetized biosorbents outperform non-magnetized systems in terms of adsorption efficiency, reusability, and operational feasibility. The review also addresses scale-up challenges, including nanoparticle leaching, regulatory compliance, and production costs, and highlights potential solutions such as green synthesis, MOF-biomass hybrids, and modular reactor designs. Overall, magnetized biosorbents represent a scalable, cost-effective, and environmentally responsible approach for industrial wastewater remediation, aligning with global sustainability goals.

Received 10th September 2025
Accepted 8th December 2025

DOI: 10.1039/d5ra06823a

rsc.li/rsc-advances

1 Introduction

The rapid pace of industrialization, particularly across the textile, paper, plastics, and leather sectors, has resulted in the large-scale discharge of synthetic dyes into aquatic environments, creating substantial risks for ecosystem integrity and public health.[1] It is estimated that nearly 10–15% of the total global production of synthetic dyes—representing several thousand tons annually—is lost to wastewater streams during manufacturing and processing operations.[2] Owing to their complex aromatic frameworks and pronounced chemical stability, these dyes exhibit strong resistance to natural degradation, leading to long-term environmental persistence.[3] Their vivid coloration compromises the visual quality of water bodies and restricts light penetration, thereby suppressing photosynthetic activity and reducing dissolved oxygen concentrations essential for aquatic life.[4] Beyond ecological consequences, many synthetic dyes exhibit toxic, mutagenic, and carcinogenic properties, raising serious concerns related to bioaccumulation and chronic human exposure through contaminated water sources.[5] As a result, the development of sustainable and efficient strategies for the removal of synthetic dyes from industrial effluents has become a central focus of contemporary water treatment and environmental protection efforts.[6]

Conventional treatment technologies such as coagulation–flocculation, biological processes (*e.g.*, activated sludge systems), advanced oxidation processes (AOPs), chemical precipitation, and membrane filtration have been widely employed for dye remediation.[7] However, their large-scale implementation faces significant challenges. Biological treatments are often insufficient against synthetic dyes due to their xenobiotic, recalcitrant molecular structures, resulting in incomplete or slow degradation.[8] Coagulation and chemical precipitation can efficiently remove dyes but generate a large volume of secondary sludge, increasing disposal costs and environmental burden.[9] Although membrane technologies offer high removal efficiencies, they are prone to fouling and require high energy input, and costly maintenance.[10] Moreover, most conventional processes depend heavily on chemical reagents or energy-intensive operations, limiting their sustainability—particularly in developing economies where cost-effectiveness and environmental compliance are critical.[11] These limitations

[a]*Department of Applied Chemistry, Faculty of Engineering and Technology, Aligarh Muslim University, Aligarh, 202002, India*
[b]*Department of Biosciences, Integral University, Lucknow, Uttar Pradesh-226026, India*
[c]*Marwadi University Research Center, Department of Agriculture, Faculty of Science, Marwadi University, Rajkot-360003, Gujrat, India. E-mail: gd4858@myamu.ac.in*

underscore the need for alternative treatment methods that are efficient, economical, and environmentally sustainable.

Adsorption has emerged as one of the most promising and versatile methods for dye removal due to its simplicity, scalability, and effectiveness in eliminating diverse type dyes.[12] Activated carbon remains the benchmark adsorbent because of its high porosity, large surface area, and excellent sorption capacity.[13] However, its high production cost, limited reusability, and environmental concerns associated with its synthesis and disposal restrict its large-scale application.[14] In contrast, plant-based adsorbents have gained attention as sustainable, low-cost alternatives.[15] Lignocellulosic biomass derived from agricultural and forestry wastes—such as coconut husks, rice husks, sawdust, fruit shells, and banana peels—contains functional groups like hydroxyl, carboxyl, and phenolic moieties that interact with dye molecules through hydrogen bonding, ion exchange, and electrostatic attraction.[16] Utilizing these bio-based materials not only enhances cost-effectiveness but also supports circular economy principles by converting agricultural and industrial residues into value-added products.[17] Although raw plant-based adsorbents are eco-friendly and effective, their industrial application is limited by several operational drawbacks, including low mechanical strength, slow adsorption rates, instability under variable effluent conditions, and difficulties in recovery and reuse.[18] Fine, powdery biosorbents often require additional filtration or sedimentation steps for separation from treated water, increasing energy demand and operational complexity.[19]

To overcome these limitations, recent research has focused on material innovations, particularly, magnetic functionalization, which emerged as a promising strategy.[20] This approach involves incorporating magnetic nanoparticles—typically magnetite (Fe_3O_4) or maghemite (γ-Fe_2O_3)—into plant derived adsorbents.[21] Magnetic cores enable rapid and efficient separation of adsorbents from wastewater using external magnetic fields, eliminating the need for energy-intensive filtration or centrifugation and enhancing reusability.[22] Additionally, magnetic nanoparticles increase surface area, active sites, and sorption kinetics, leading to high dye removal efficiencies across various dye classes.[23] The synthetic interactions between biomasses functional groups and magnetic cores further strengthens electrostatic attraction, π–π stacking, and hydrogen bonding, improving overall adsorption performance.[24] Moreover, surface modifications such as amination or carboxylation can be integrated with magnetization to enhance selectivity and adaptability toward specific dye chemistries, expanding industrial applicability.[25]

The development of magnetized plants-based adsorbents represents a significant advancement in sustainable wastewater treatment, bridging the gap between environmental friendliness and technological efficiency.[26] These hybrid materials retain the biodegradability and renewability of their biomass origin while overcoming major operational challenges such as recovery, regeneration, and scalability.[27] As industries face increasing pressure to comply with stringent environmental standards, magnetized biosorbents offer a practical, scalable, and eco-friendly alternative to conventional treatment technologies.[28]

This review aims to comprehensively explore potential of plant-based adsorbents as magnetized materials for industrial dye removal, with emphasis on their synthesis, structural functionality, and practical applications. It further examines magnetic functionalization methods involving NPs incorporation, surface modification, evaluating their effects on adsorption capacity, kinetics, and recyclability. The review also discusses current challenges and future prospects to assess large-scale feasibility of these materials.

2 Dye pollution and its environmental impact

The widespread use of synthetic dyes in industrial wastewater represents one of the most persistent environmental challenges of the past century.[29] Global dye production exceeds one million tons annually, primarily driven by the textile, leather, plastics, paper, food, and cosmetics industries.[30] During manufacturing and processing, an estimated 10–15% of these dyes are lost and discharged into aquatic systems as untreated or partially treated effluents.[31] Owing to their complex aromatic structures and high stability, these dyes resist photolytic and microbial degradation, enabling their persistence in water bodies.[32] Their accumulation reduces light penetration, disrupts photosynthesis, lowers dissolved oxygen levels, and destabilizes aquatic ecosystems.[33] Furthermore, many dyes and their degradation products exhibit mutagenic, carcinogenic, or endocrine-disrupting properties, posing serious risks to human and environmental health.[34]

2.1 Sources of dyes in industrial wastewater

Industrial wastewater contaminated with dyes originates from several key sectors, with the textile industry alone contributing nearly 60–70% of global dye discharge.[35] Textile dyeing and finishing consumes large volumes of water, and inefficient dye-fiber fixation—often below 50% for reactive dyes—results in substantial dye losses during washing and rinsing.[36] Other major contributors include the leather industry, which employs basic and reactive dyes for tanning and finishing.[37] The paper and pulp sector, which uses direct and reactive dyes for paper coatings; and the plastics and printing industries, where solvent and pigment dyes are used extensively.[38] Small-scale and informal industries often release untreated or poorly treated effluents due to high operational costs of conventional treatment systems.[39] Additionally, dyes enter water systems through degradation of consumer products, improper disposal of coloured materials, and leachates from landfills containing dye-laden waste.[40] Their persistence in wastewater is primarily attributed to structural features—such as azo linkages (–N=N–), sulfonic groups, and halogen substitutions—that confer stability and resistance to biodegradation.[41] As illustrated in Fig. 1, dye pollution arises from diverse industrial and domestic sources, with azo, reactive, and basic dyes posing significant ecological and toxicological threats that necessitate sustainable regulatory control.

2.2 Toxicological profile of major dye classes

Synthetic dyes comprise several chemical classes, among which, azo, reactive dyes, and basic dyes—are most significant due to

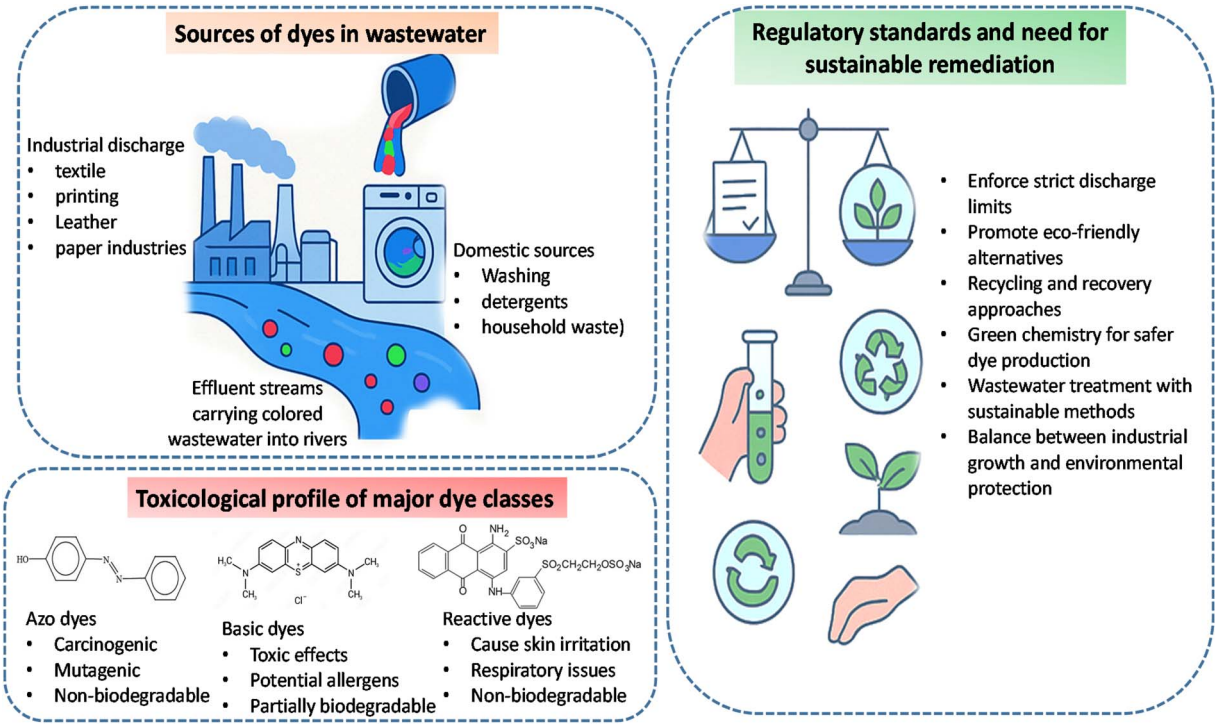

Fig. 1 Sources, toxicological profiles, and regulatory considerations of dye pollution in wastewater. Industrial and domestic activities contribute to dye release into aquatic environments. Azo dyes exhibit carcinogenic and mutagenic effects, reactive dyes cause dermal and respiratory issues, while basic dyes are linked with toxicity and allergenicity. The figure also emphasizes the urgent need for sustainable remediation strategies, strict.

their high production volume, persistence, and toxicological risks.[42] Each group exhibits distinct chemical properties that determines its behaviour in the environment and its and biological impacts. Azo dyes, containing one or more azo linkages (–N=N–), accounts for nearly 60–70% of global dye use because of their vivid colours, versatility, and low cost.[43] However, they are also among the most persistent pollutants, resisting photolytic and microbial degradation. Under anaerobic conditions, they can undergo reductive cleavage to form aromatic amines, compounds known for their mutagenic and carcinogenic potential.[44] Studies have linked azo dyes such as Congo red and Direct black-38 to genotoxicity and cytotoxicity, and increased risks of bladder and liver cancers in humans and animals.[45,46] Ecologically, azo dyes accumulate in sediments, disrupt microbial communities, and cause reproductive toxicity in fish.[47]

Reactive dyes form covalent bond with cellulose fibers, yielding bright and wash-fast colors.[48] Despite these advantages, dye-fiber fixation is often below 50%, leading to substantial losses in effluent.[49] Their structural features such as sulfonic acid groups, halogenated chromophores, and reactive moieties (*e.g.*, monochlorotriazine) enhance solubility but make them highly resistant to biodegradation.[50] Reactive dyes have been associated with allergic dermatitis and respiratory sensitization in exposed workers[51] and with inhibition of algal growth, reduced photosynthetic oxygen production, and trophic imbalance in aquatic ecosystems.[52]

Basic (cationic) dyes, including methylene blue and crystal violet, are extensively used in paper, leather, and acrylic fiber industries.[53] Their high tinctorial strength and solubility contribute to persistent in wastewater.[54] Toxicological studies indicate that dyes induce cytotoxicity, oxidative stress, DNA damage in mammalian cells.[55] In aquatic systems, cationic dyes strongly adsorb to negatively charged elements or biota, leading to bioaccumulation and toxicity in fish and benthic organisms.[56] Notably, crystal violet is classified as a potential carcinogen due to its mutagenic behaviour in microbial and mammalian systems.[57] An overview of industrial sources, persistence, toxicological effects, and regulatory aspects of major dye classes—including azo, reactive, and basic dyes—is summarized in Table 1.

2.3 Regulatory standards and need for sustainable remediation

The environmental and toxicological risks associated with dye pollution have led regulatory authorities worldwide to impose stringent discharge standards. The World Health Organization (WHO) and United States Environmental Protection Agency (USEPA) have set maximum permissible limits for several dyes and their degradation products due to their carcinogenic and mutagenic potential.[68] In India, the Central Pollution Control Board (CPCB) enforces chemical oxygen demand (COD) levels below 250 mg L^{-1} and mandate zero visible coloration in treated effluents released into surface waters.[69] Similarly, under the European Union's Integrated Pollution Prevention and Control (IPPC) framework and related water-quality legislation, several azo-derived aromatic amines are classified as hazardous

Table 1 Industrial sources, compounds, environmental persistence, toxicological effects, and general effluent organic load limits[a]

Dye class	Representative compounds	Primary industrial sources	Environmental persistence	Typical environmental concentrations (μg L^{-1}–mg L^{-1})	Toxicological effects	General effluent standards (COD/BOD)	Ref.
Azo dyes	Methyl orange, Direct red 8r	Textile dyeing, leather, food processing	Highly recalcitrant; resistant to biodegradation due to –N=N– bonds	5–200 μg L^{-1} in river water near textile clusters; up to 1–5 mg L^{-1} in untreated effluent	Mutagenic, carcinogenic (*via* aromatic amines)	Restricted by EU REACH; monitored by USEPA and CPCB	58 and 59
Azo dyes	Acid orange-7, Congo red	Paper printing, cosmetics, textile finishing	Stable in wastewater; forms toxic aromatic amines under anaerobic conditions	10–150 μg L^{-1} in surface water; 0.5–3 mg L^{-1} in dye-house influent	Endocrine disruption; hepatotoxicity in humans	Banned or limited in EU and India (*e.g.*, Congo red)	60 and 61
Reactive dyes	Reactive blue 19, Reactive black-5	Cotton and synthetic fiber dyeing, textile printing	Moderately persistent; hydrolyze slowly; may disrupt aquatic photosynthesis	20–300 μg L^{-1} in receiving waters; 1–20 mg L^{-1} in textile wastewater	Cytotoxic to algae and invertebrates; may cause gill damage in fish	Regulated under EU water quality directives; effluent COD limits apply	62
Reactive dyes	Reactive red 120, Reactive yellow 145	Wool, silk, and nylon dyeing, wastewater from finishing plants	High water solubility; persistent color in effluents	10–200 μg L^{-1} in rivers; 0.3–5 mg L^{-1} in industrial wastewater	Skin and eye irritation; chronic exposure linked to liver stress	Subject to local discharge standards (0.1–1 mg L^{-1} typical)	63
Basic dyes	Methylene blue, crystal violet	Textile finishing, paper printing, medical staining	High solubility and mobility; bind strongly to organic matter	<1–20 μg L^{-1} in natural waters; 0.5–10 mg L^{-1} in effluent	Neurotoxicity and genotoxicity; causes oxidative stress	Controlled under WHO and USEPA aquatic toxicity guidelines	64 and 65
Basic dyes	Basic red 46, malachite green	Plastics, leather, aquaculture antifungal treatments	Persistent; bioaccumulate in aquatic species	<1–10 μg L^{-1} in lakes/rivers; 0.2–3 mg L^{-1} in aquaculture discharge	DNA damage; carcinogenic potential in rodents	Banned for food contact by FDA; regulated in textile discharges	66 and 67

[a] COD limits indicate the maximum allowable total organic load in treated effluents. These values do not represent dye-specific regulatory limits, but they indirectly constrain dye discharge because reactive dyes contribute significantly to the overall organic burden of wastewater.

or high-concern substances due to their mutagenic or carcinogenic potential. Although these designations do not constitute compound-specific discharge limits, they underscore the need for stringent monitoring and effective treatment to minimise their release into aquatic environments.

Despite these regulations, compliance remains difficult with conventional treatment methods, which often suffer from high operational costs, excessive sludge generation, and incomplete pollutant removal—particularly in resource-limited regions. This challenge highlights the need for sustainable, low-cost, and scalable alternatives. In recent years, plant-based biosorbents and their magnetic functionalization have emerged as promising solutions, offering high adsorption efficiency, easy recovery, and alignment with green chemistry principles.[70] Such innovations not only overcome the limitations of traditional systems but also advance circular economy objectives by utilizing renewable, biodegradable materials to mitigate persistent dye pollutants.

3 Plant-based adsorbents: composition and mechanisms

The use of plant-based adsorbents for dye removal has gained significant attention owing to their abundance, low cost, renewability, and chemical versatility. These biomaterials are rich in structural polysaccharides, lignin, and secondary metabolites, which collectively enhance their adsorption capacity.[71] The abundant functional groups and a porous structure enables interaction with a wide range of dyes through various physicochemical mechanisms. A thorough understanding of their composition and adsorption behaviour is crucial for optimizing and customizing these materials for industrial wastewater treatment applications.

3.1 Structural composition of biomass

Plant biomass primarily comprises three major biopolymers—cellulose, hemicellulose, and lignin—along with various phytochemicals, each contributing distinctively to dye adsorption behaviour.[72] Together, these components form a heterogeneous, functionalized matrix capable of binding dyes through electrostatic interactions, hydrogen bonding, hydrophobic effects, and π–π stacking.[73]

Cellulose, the most abundant organic polymer on Earth, is a linear β-(1 → 4)-linked D-glucose polysaccharide organized into microfibrils that provide high surface area and mechanical strength.[74] Its abundant hydroxyl groups act as active sites for hydrogen bonding and polar interactions with dye molecules.[75] Natural cellulose-rich materials such as rice husks and cotton stalks have shown over 70% dye removal efficiency, while chemical modifications—such as carboxylation or amination—further enhance selectivity and adsorption capacity.[76]

Hemicellulose consists of branched polysaccharides like xylans, mannans, and arabinogalactans, which are more amorphous and hydrophilic than cellulose.[77] Although it contributes less to structural rigidity, its reactive hydroxyl and carboxyl groups that act as effective anchoring sites for ionic dyes, while its amorphous structure promotes water swelling and diffusion. For instance, sugarcane bagasse, rich in hemicellulose, exhibits strong adsorption of acidic dyes through ion exchange.[78]

Lignin, a complex aromatic polymer, serves as a natural binder within cell lays a key role in adsorbing hydrophobic and aromatic dyes.[79] Its phenolic and methoxy groups facilitate π–π interactions and hydrophobic bonding with aromatic dye molecules such as azo and basic dyes. Lignin-rich materials like sawdust and wood chips display high adsorption capacities for cationic dyes (*e.g.*, methylene blue) through electrostatic attraction between dye amine groups and negatively charged lignin surfaces at neutral to alkaline pH.[80]

Beyond structural polymers, plant residues contain diverse secondary metabolites—including tannins, flavonoids, saponins, and organic acids—that enhance dye binding by providing additional active sites or modifying surface chemistry.[81] Tannins, in particular, exhibit strong dye-binding ability *via* polyphenolic chelation and hydrophobic interactions.[82] Tannin-rich bark adsorbents have demonstrated rapid uptake of both basic and reactive dyes, underscoring the synergistic role of phytochemicals in adsorption processes.[83]

Overall, structural and chemical diversity of lignocellulosic biomass—spanning cellulose, hemicellulose, lignin, and bioactive phytochemicals—provides multiple functional groups and interaction mechanisms that underpin the efficiency of plant-based adsorbents.[84] Table 2 summarizes their key compositional features, while Fig. 2 illustrates their functional roles and adsorption mechanisms.

3.2 Natural adsorption mechanisms

The interaction between plant-based adsorbents and dye molecules is governed by a combination of electrostatic attractions, hydrogen bonding, and van der Waals forces, often working synergistically to achieve efficient pollutant removal.

Electrostatic attraction is a dominant mechanism for many plant-based systems, particularly when surface functional groups (*e.g.*, carboxylates, hydroxyls, phenolics) acquire charges depending on solution pH.[93] For cationic dyes like crystal violet and methylene blue, negatively charged surfaces (achieved at neutral or basic pH) facilitate strong binding through coulombic forces.[94] Conversely, protonated biomass surfaces at acidic pH can attract anionic dyes such as Congo red or Reactive black 5. Multiple studies[95] have shown that optimizing solution pH to match the charge profiles of dyes and adsorbents can enhance removal efficiencies by up to 50%.

Hydrogen bonding occurs between electronegative atoms (oxygen, nitrogen) in the dye molecules and hydrogen donors present in the biomass, particularly the hydroxyl groups of cellulose and hemicellulose.[96] This mechanism is particularly important for reactive and azo dyes containing amine or hydroxyl groups that can serve as hydrogen bond donors or acceptors. Hydrogen bonding not only aids initial adsorption but also stabilizes dye molecules within the biomass matrix, enhancing uptake even at low concentrations.[97]

Although weaker than electrostatic interactions and hydrogen bonding, van der Waals forces contribute to the adsorption of non-polar or weakly polar dye molecules.[98] These forces, combined with hydrophobic interactions, enable lignin-rich biomass to adsorb aromatic dyes effectively. For instance, wood-derived adsorbents with high lignin content demonstrate strong affinity toward hydrophobic dyes like disperse blue,

Table 2 Structural composition of lignocellulosic biomass, chemical structure, functional groups, adsorption roles, natural abundance, and typical sources of cellulose, hemicellulose, lignin, and phytochemical constituents

Component	Chemical structure	Functional groups	Role in dye adsorption	Abundance in biomass (%)	Source examples	Ref.
Cellulose	Linear chains of β-(1 → 4)-linked D-glucose units; crystalline microfibrils	Hydroxyl (–OH); capable of hydrogen bonding	Forms H-bonds with polar dyes and attracts cationic dyes when deprotonated	30–50% (varies by plant source)	Cotton fibers, rice husk, banana peels, sugarcane bagasse	85 and 86
Hemicellulose	Branched heteropolymers of pentoses (xylose, arabinose) and hexoses (mannose, glucose)	Carboxyl (–COOH), hydroxyl (–OH), acetyl ($–COCH_3$) groups	Carboxylates enable ion exchange, electrostatic binding, and enhance hydrophilicity for aqueous uptake	15–35% depending on species	Corn stover, wheat straw, fruit peels, coconut coir	87 and 88
Lignin	Amorphous, three-dimensional aromatic polymer of phenylpropanoid units (*p*-coumaryl, coniferyl, sinapyl alcohols)	Phenolic (–OH), methoxy ($–OCH_3$), aromatic rings (π systems)	π–π stacking and hydrophobic-van der Waals interactions enhance non-polar dye adsorption	15–30% in hardwoods and softwoods	Wood chips, bark residues, sawdust, coconut shells	89 and 90
Phytochemical components	Polyphenols, tannins, flavonoids, alkaloids, and terpenoids present in minor quantities	Hydroxyl, carboxyl, amine ($–NH_2$), and aromatic moieties	Chelates metal-dye complexes and aids adsorption *via* radical scavenging and H-bonding	Typically <5%, varies widely by species and processing	Tea leaves, eucalyptus, neem bark, grape skins	91 and 92

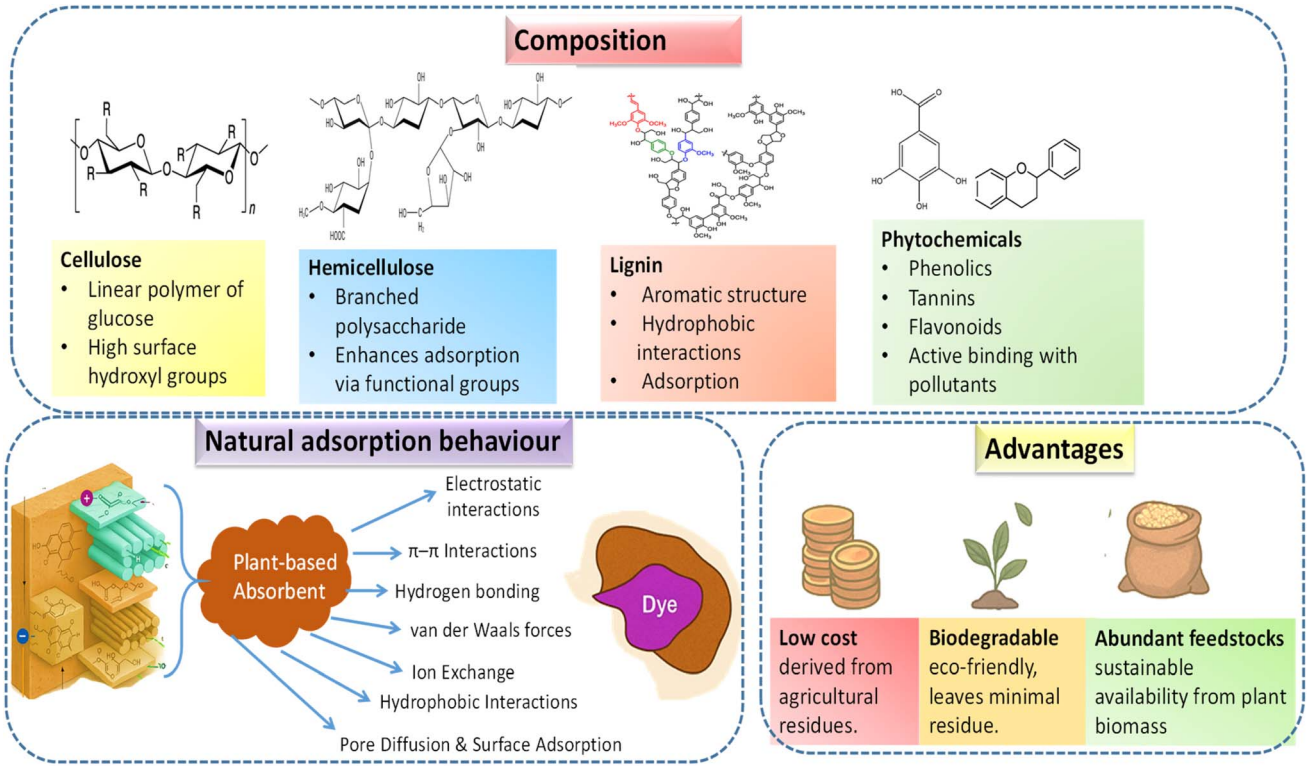

Fig. 2 Structural composition and adsorption mechanisms of plant-based adsorbents. Cellulose, hemicellulose, lignin, and phytochemicals provide diverse functional groups that facilitate adsorption. Natural mechanisms involve electrostatic interactions, hydrogen bonding, van der Waals forces, π–π stacking, ion exchange, hydrophobic interactions, and complexation with pollutants. These properties, combined with their low cost, biodegradability, and abundant availability, make plant-based adsorbents a sustainable alternative for wastewater treatment.

driven by π–π stacking and London dispersion forces.[99] These natural mechanisms often act in concert, with their relative contributions influenced by dye chemistry, solution pH, ionic strength, and the surface properties of the adsorbent.

3.3 Advantages of plant-based adsorbents

The use of plant-derived materials as adsorbents offers several distinct advantages that make them attractive alternatives to conventional sorbents such as activated carbon. Agricultural residues and forestry by-products are readily available and often treated as waste, incurring disposal costs. Although converting biomass residues into adsorbents offers a cost-effective approach for dye removal, this benefit must be balanced against the environmental implications associated with their full life cycle, including the fate of spent material.[100] For instance, sugarcane bagasse and coconut coir, available in abundance in tropical regions, have been successfully utilized for removing dyes like malachite green and methylene blue, with adsorption capacities comparable to commercial activated carbon.[101]

Unlike synthetic adsorbents or chemically intensive systems, plant-based materials are biodegradable, minimizing the risk of secondary pollution.[102] Post-adsorption, these materials can often be composted, incinerated, or regenerated with relatively low environmental impact. This aligns with green chemistry and circular economy principles, where waste valorisation is central to sustainable industrial practices. The global generation of agricultural waste exceeds billions of tons annually, encompassing rice husks, fruit peels, nut shells, sawdust, and more.[103] This widespread availability ensures a steady and scalable feedstock supply for adsorbent production. Moreover, region-specific biomass can be tailored to local industries, reducing transportation costs and enhancing the feasibility of decentralized wastewater treatment solutions.

4 Magnetization techniques and functionalization

4.1 Synthesis of magnetic nanoparticles (MNPs)

The most commonly used magnetic materials in the manufacture of magnetized plant-based adsorbents are magnetic nanoparticles (MNPs), especially iron oxide-based materials, including magnetite (Fe_3O_4) and maghemite (γ-Fe_2O_3).[104] They are the best options to use in environmental remediation due to their superparamagnetic properties, chemical stability, and relatively low toxicity.[105] Their crystal size, surface chemistry, saturation magnetization, and dispersibility all directly depend on the synthesis method and will affect their performance when used with biomass.[106] Out of many methods, the most common include co-precipitation, sol–gel, and hydrothermal synthesis, as they are simple to use, can be scaled, and produce tunable nanoparticles.[107]

The most popular method to prepare Fe_3O_4 nanoparticles is co-precipitation which is simple, cheap, and scalable.[108] In this process, ferric (Fe^{3+}) and ferrous (Fe^{2+}) salts, typically chlorides or sulfates, are dissolved in water and precipitated by adding

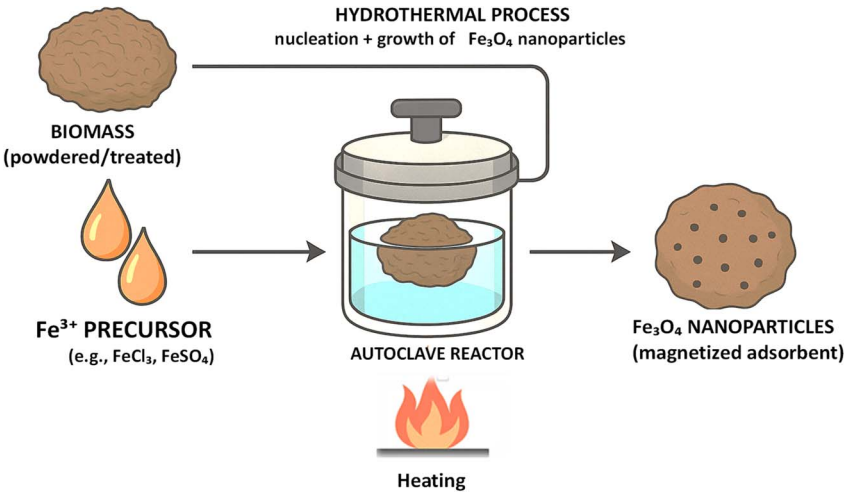

Fig. 3 Schematic representation of the hydrothermal synthesis route, where biomass and an Fe^{3+} precursor is combined in an autoclave and heated to yield Fe_3O_4-loaded material.

a base such as sodium hydroxide (NaOH) or ammonium hydroxide (NH_4OH) under an inert atmosphere.[109] The reaction can be expressed as:

$$Fe^{2+} + 2Fe^{3+} + 8OH^- \rightarrow Fe_3O_4 + 4H_2O$$

The precipitation must be carried out under carefully controlled pH (generally between 9 and 11), temperature, and oxygen-free conditions to avoid oxidation of magnetite (Fe_3O_4) to maghemite (γ-Fe_2O_3). The adhesion of particles and their crystallinity can be tailored by changing the following factors: the Fe^{2+}/Fe^{3+} ratio, ionic strength and the temperature of the reaction. The pioneer of this technique showed that nanoparticles of 5 to 20 nm could be easily prepared by regulating the following parameters.[110] Recent studies have optimized co-precipitation in the environment. To illustrate, Fe_3O_4 nanoparticles were prepared through this process and coated on rice husk biochar with 92% removal of methylene blue in aqueous solutions.[111] Although this procedure has the benefit of not necessitating high-temperature treatment, it may result in polydisperse nanoparticles and will commonly necessitate the subsequent stabilization of the product by addition of surfactants (*e.g.*, citric acid) to prevent agglomeration, which is notably significant when integrating into plant-based adsorbents.

Sol–gel technique is a process in which metal alkoxides are hydrolysed and poly-condensed in a solvent system, which leads to formation of a colloidal sol, which can later be dried and gelled into Fe_3O_4 nanoparticles.[112] With better particle size distribution, morphology and crystallinity control over co-precipitation, the method is preferred in areas of necessity where uniform nanoparticles with a desired surface functionality are needed.[113] In sol–gel synthesis, the nucleation and growth processes are controlled by parameters like the precursor concentration, water-to-alkoxide ratio, pH and aging time.[114] The process is then usually followed by calcination at moderate temperatures (300–600 °C), which promotes crystallization of iron oxides.[115] Although calcination enhances crystallinity and magnetic properties, it may increase particle size, thereby reducing surface area and adsorption capacity. Previous research has also demonstrated the advantages of sol–gel synthesis in producing stable and functionalized Fe_3O_4 nanoparticles.[116] Sol–gel-derived Fe_3O_4-silica hybrids have also been reported to significantly enhance adsorption performance when used to magnetically modify biomass-derived carbons.[117]

Hydrothermal synthesis involves crystallizing Fe_3O_4 nanoparticles in sealed autoclaves at elevated temperatures (typically 120–250 °C) and autogenous pressures, using aqueous solutions of iron salts, often in the presence of structure-directing agents or surfactants.[118,119] This method produces highly crystalline and monodisperse Fe_3O_4 nanoparticles without the need for post-calcination, making it particularly suitable for fabricating magnetic biomass composites.

4.2 Integration of magnetic nanoparticles with biomass

The successful development of magnetized plant-based adsorbents hinges on the efficient immobilization of magnetic nanoparticles (MNPs) onto or within biomass matrices. This hybridization imparts magnetic responsiveness to otherwise non-magnetic biopolymers, allowing for facile separation post-adsorption *via* external magnetic fields.[120] The integration also improves dispersion, enhances surface area, and, when tailored appropriately, can synergize with the biomass's inherent functional groups to increase dye-binding capacity. A wide array of agricultural and forestry residues has been used as biosorbent matrices for magnetic nanoparticle incorporation.[121] Among these, leaves, fruit peels, tree bark, and agro-wastes such as husks and stalks are particularly attractive due to their lignocellulosic composition, low cost, and surface reactivity.[122]

Fruit peels (*e.g.*, banana, orange, pomegranate) are rich in cellulose and pectin, providing hydroxyl and carboxylic acid groups that facilitate the anchoring of Fe_3O_4-NPs *via* hydrogen bonding and electrostatic interactions.[123] For example, Fe_3O_4-banana peel biochar composites fabricated using co-precipitation achieved over 95% removal of crystal violet and methylene blue within 60 min, where the natural porosity of peels improved

nanoparticle dispersion and increased active surface area.[124] Tree bark—particularly from species like neem, eucalyptus, and pine—is another promising candidate, as it contains polyphenols, tannins, and lignin with high affinity for both dyes and MNPs. Pine bark modified with Fe_3O_4 showed enhanced removal of anionic dyes like Congo red due to π–π stacking interactions and magnetic enrichment of adsorption sites.[125]

Leaf biomass such as eucalyptus and guava leaves has also been used due to its surface functionalization potential after drying and pyrolysis. Magnetized leaf powder composites prepared *via* hydrothermal deposition of Fe_3O_4 resulted in efficient sorption of reactive dyes and reusability across multiple cycles.[126] Agro-industrial wastes like rice husk, wheat straw, coconut coir, and corn stover are particularly advantageous for large-scale applications, offering structural robustness and wide availability.[127] These substrates often undergo carbonization (biochar formation) prior to magnetization, enhancing both surface area and thermal stability. Magnetized corn stover biochar prepared *via in situ* Fe_3O_4 growth reported adsorption capacities over 150 mg g^{-1} for methylene blue, significantly outperforming raw biomass.[128]

Integration of magnetic nanoparticles into plant-based biomass is commonly achieved through three main approaches. *In situ* precipitation involves precipitating Fe^{2+}/Fe^{3+} salts directly onto the biomass under alkaline conditions, allowing nanoparticles to anchor within the matrix.[129] Physical mixing with sonication disperses pre-synthesized nanoparticles uniformly across the biomass surface, enhancing coverage and stability. Hydrothermal embedding subjects the biomass and iron precursors to elevated temperature and pressure, promoting strong chemical bonding and uniform nanoparticle incorporation.[130] Together, these techniques enhance the magnetic properties, stability, and adsorption efficiency of the resulting composites. The method of integration affects nanoparticle stability, leaching behaviour, and surface accessibility—all key parameters for consistent adsorption performance.[131]

Post-integration, these composites often undergo functionalization treatments to further enhance dye uptake capabilities. The synthesis routes and integration strategies for magnetic nanoparticles, along with their optimal conditions, advantages, and limitations, are summarized in Table 3. This compilation highlights how co-precipitation, sol–gel, hydrothermal synthesis, and biomass integration approaches have been optimized to produce efficient, stable magnetized adsorbents for wastewater treatment applications.

4.3 Surface modification strategies

To enhance adsorption performance, magnetized plant-based biosorbents are commonly subjected to surface modification techniques that tailor their physicochemical properties. Such

Table 3 Synthesis methods and integration techniques for magnetic nanoparticles

Technique	Process description	Key advantages	Limitations	Optimal conditions	Reported applications	Ref.
Co-precipitation	Co-precipitation of Fe^{2+}/Fe^{3+} in alkaline medium (pH 9–11) under inert atmosphere at 25–80 °C	Simple, scalable, cost-effective; widely used for large-scale Fe_3O_4 production	Polydispersity; requires stabilizers (citric acid, surfactants); risk of oxidation	pH 9–11; 1 : 2 Fe^{2+}/Fe^{3+}; N_2 atmosphere; 25–80 ° C	Fe_3O_4-rice husk biochar for methylene blue and Congo red removal	132
Sol–gel process	Sol–gel hydrolysis and condensation of iron precursors, followed by drying and calcination (300–600 °C)	Produces uniform, tunable nanoparticles; allows surface functionalization	Complex, energy-intensive; uses organic solvents and calcination	Acidic to neutral pH; drying and calcination at 300–600 °C	Fe_3O_4-coated silica composites for arsenic and dye adsorption	133
Hydrothermal synthesis	Hydrothermal treatment of iron precursors (120–250 °C) yields crystalline, size-controlled Fe_3O_4	Highly crystalline, stable particles; precise control over size and shape	Slow, energy-intensive; requires specialized autoclaves	Autoclave temperatures 120–250 °C; reaction time 4–24 h	Magnetized biochar for heavy metals and dye removal	134
In situ precipitation on biomass	Fe^{2+}/Fe^{3+} co-precipitated on biomass surfaces for strong anchoring and uniform Fe_3O_4 dispersion	Strong attachment of nanoparticles; minimizes leaching; eco-friendly	pH-sensitive; requires inert conditions; can alter biomass structure	Alkaline medium; mild temperatures (<80 °C); biomass pre-treatment	Fe_3O_4-sugarcane bagasse composites for Reactive black 5	135
Physical mixing & sonication	Sonication of nanoparticles with biomass ensures uniform coating; citric acid prevents aggregation	Uniform nanoparticle dispersion; compatible with diverse biomasses	Possible nanoparticle detachment during cycles; needs surfactant aid	Room temperature mixing; ultrasonic energy (20–40 kHz)	Fe_3O_4-orange peel composites for cationic dye removal	136
Hydrothermal embedding	Thermal reaction of biomass with iron precursors embeds nanoparticles *via* covalent bonding	High stability and binding strength; improved durability for repeated use	More costly; high-pressure setup needed; scalability challenges	Biomass soaked in iron precursor and treated at 120–200 °C for 6–12 h	Fe_3O_4-wood chip composites for mixed dye effluents	137

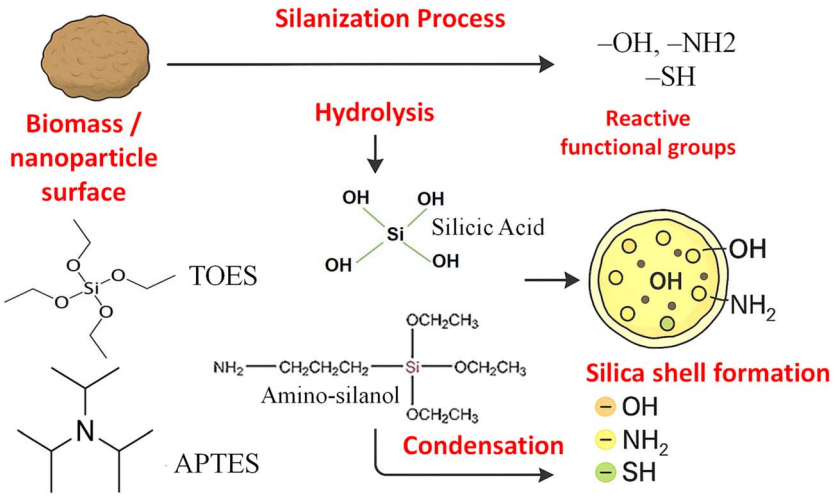

Fig. 4 Schematic representation of the silanization process, illustrating hydrolysis and condensation of TEOS/APTES and subsequent grafting of a silica shell enriched with reactive –OH, $–NH_2$, and –SH groups on the biomass or nanoparticle surface.

treatments introduce new functional groups, alter surface charge, and modulate hydrophilicity or hydrophobicity depending on target pollutant. Among these, acid/alkali activation, silanization, and polymer grafting are most widely employed strategies.

Alkaline activation using NaOH or KOH removes impurities and lignin, expose cellulose fibrils, and generate phenolic hydroxyl groups that facilitate hydrogen bonding and ion exchange interactions.[138] NaOH-pre-treated coconut coir showed nearly double the adsorption capacity for Reactive red 120 relative to untreated biomass.[139] Acid-activated similarly surface charge and active-site density; for instance, Fe_3O_4-impregnated mango seed kernel powder treated with acid exhibited markedly higher methylene blue removal.[140]

In magnetic biosorbents, these activations steps are typically carried out before or immediately after nanoparticle incorporation to improve both nanoparticle anchoring and dye-binding efficiency.[141] However, excessive treatment can weaken the biomass structure or promote nanoparticles leaching, underscoring the need to carefully optimise reagent concentration and reaction time.

Silanization involves the modification of biomass or nanoparticle surfaces using organosilanes such as tetraethyl orthosilicate (TEOS) or 3-aminopropyltriethoxysilane (APTES), forming a silica shell that enhances structural stability and introduces reactive functional groups (–OH, $–NH_2$, –SH).[142] The overall process—comprising hydrolysis, condensation, and surface grafting—is illustrated schematically in Fig. 4. This strategy is particularly useful in preventing nanoparticle aggregation, improving dispersibility, and providing anchoring points for further modification. Fe_3O_4@-SiO_2 particles immobilized onto peanut shell-derived carbon exhibited over 90% removal of Congo red and maintained sorption efficiency over five regeneration cycles.[143] APTES-modified biosorbents have also shown strong affinity for anionic dyes through amine–sulfonic acid interactions, increasing selectivity in mixed-dye wastewater systems. Silanization is typically done under mild conditions (alcohol–water mixture, pH 4–5), ensuring compatibility with the fragile biomass matrix. It is often followed by cross-linking or polymer grafting to enhance robustness.[144]

Polymer grafting is an effective strategy to enhances both adsorption capacity and dye selectivity by introducing functional polymer chains onto the biosorbent surface. Depending on the dye targeted classes, these polymers can impart cationic functionalities (*e.g.*, poly-ethylenimine, chitosan) or anionic groups (*e.g.*, polyacrylic acid), thereby improving electrostatic interactions and binding affinity.[145]

Chitosan-grafted magnetic biochar has received particular attention because chitosan is biodegradable, film-forming, and rich in amine groups that strongly interact with anionic dyes.[146] For instance, a chitosan-Fe_3O_4-biochar composite prepared from sugarcane bagasse achieved 98% removal of methyl orange and maintained high regeneration efficiency over six adsorption–desorption cycles.[147]

Synthetic polymers such as polyacrylamide or poly-ethylenimine have also been applied to increase the density of functional groups and enhance dye selectivity.[148] Grafting can be achieved through free radical polymerization, UV activation, or coupling reaction using agents such as EDC/NHS in aqueous media.[149] Although polymer grafting substantially improves performance, it may reduce biodegradability and increase material cost. Consequently, recent efforts focus on hybrid approaches that combine natural polymers with bio-based grafting agents, aiming to balance adsorption efficiency with environmental sustainability.

4.4 Green synthesis approaches for Fe_3O_4-NPs

In addition to conventional physical and chemical routes such as co-precipitation and hydrothermal synthesis, increasing attention has been directed toward green synthesis methods that utilize biological resources as reducing and stabilizing agents.[150] Plant extract-mediated synthesis employs phytochemicals such as polyphenols, flavonoids, and sugars to reduce ferric ions under mild conditions, eliminating the need for toxic solvents or harsh reducing agents.[151] Similarly, microbial synthesis using bacteria, fungi, or algae provides a sustainable alternative where

metabolites secreted by microorganisms promote *in situ* reduction and capping of Fe_3O_4-NPs.[152]

Compared with conventional methods, green synthesis offers advantages such as eco-friendliness, lower energy input, and biocompatible surface coatings that enhance stability and reduce aggregation.[153] However, limitations include less control over particle size distribution, reproducibility, and reaction kinetics, which can affect magnetic properties.[154] Integration of these biological routes with controlled physicochemical conditions may provide a promising balance between sustainability and functionality in future applications.[155]

5 Adsorption performance and mechanistic insights

The performance of magnetized plant-based adsorbents depends on their adsorption capacity, equilibrium relationships, kinetic behavior, thermodynamic feasibility, and the interaction mechanisms responsible for dye removal. Breaking down these aspects offers clarity on how such materials can be optimized for industrial wastewater treatment.

5.1 Adsorption isotherms and capacity evaluation

Adsorption isotherms describe how dye molecules distribute between the liquid and solid phases at equilibrium, providing insight into the adsorption capacity and surface characteristics of an adsorbent.[156] For magnetized plant-based materials, adsorption equilibrium is commonly described using the Langmuir and Freundlich isotherm models. The Langmuir isotherm explains adsorption as a monolayer process occurring on a uniform surface with identical, energetically equivalent sites, and assumes no interaction between adsorbed molecules.[157] This model is particularly suitable for magnetized biochar and biomass composites, where the incorporation of Fe_3O_4 nanoparticles enhances surface uniformity and creates defined active adsorption sites.[158]

The Langmuir equation is expressed as:

$$q_e = (q_{max} \times K_L \times C_e)/(1 + K_L \times C_e)$$

where q_e (mg g^{-1}) is the amount of dye adsorbed at equilibrium, q_{max} (mg g^{-1}) represents the maximum adsorption capacity corresponding to complete monolayer coverage, K_L (L mg^{-1}) is the Langmuir adsorption constant, and C_e (mg L^{-1}) is the equilibrium dye concentration. Magnetized biomass-based adsorbents have been reported to exhibit q_{max} values typically between 150 and 250 mg g^{-1} for several model dyes, with variability depending on surface chemistry, porosity, and magnetization efficiency.

In contrast, the Freundlich isotherm empirically describes adsorption on heterogeneous surfaces with sites of varying energies, allowing multilayer formation—an effect typical of lignocellulosic materials due to their diverse functional groups and porous structure.[159]

The Freundlich equation is given as:

$$q_e = K_f \times (C_e)^{(1/n)}$$

where K_f (mg g^{-1})(L mg^{-1})$^{(1/n)}$ is the Freundlich constant indicative of adsorption capacity, and $1/n$ is a dimensionless parameter reflecting adsorption intensity and favourability. When $1/n < 1$, adsorption is considered favourable.

Many magnetized plant-derived adsorbents demonstrate equilibrium data that can be fitted to both Langmuir and Freundlich models.[160] The simultaneous applicability of both models reflects the complex surface characteristics of magnetized biomass composites rather than a strict coexistence of distinct monolayer and multilayer mechanisms. In practice, the choice of the better-fitting isotherm is empirical and determined by statistical correlation coefficients ($R^2 \geq 0.98$ typically indicates a good fit) and error function analyses such as χ^2 or RMSE.[161,162] A relatively higher R^2 value for the Langmuir model suggests dominance of homogeneous surface adsorption sites, whereas comparable fits for both models may indicate surface heterogeneity introduced by the biomass matrix.

Representative adsorption constants for various magnetized plant-based adsorbents, evaluated against different dye systems, are summarized in Table 4. These values highlight the high maximum adsorption capacities and favourable Freundlich intensity factors that collectively demonstrate the strong affinity and versatility of these materials for dye remediation.

5.2 Kinetics and thermodynamics

Kinetic modelling reveals the rate and mechanism of dye uptake. The pseudo-first-order model assumes physical adsorption, where uptake depends on the difference between equilibrium capacity and current loading.[163]

The pseudo-second-order model represents chemisorption processes involving electron sharing, ion exchange, or valence interactions, and is typically more applicable to magnetized biosorbents.[173] Composites derived from sugarcane bagasse, corn stover, or banana peel, particularly when amine or carboxyl groups are introduced, frequently align with the pseudo-second-order model ($R^2 > 0.99$), signifying those chemical interactions dominate.[174]

Thermodynamic analysis complements kinetic data by establishing feasibility and energetic characteristics.[175] Negative ΔG values confirm spontaneity, while ΔH differentiates adsorption types—values of 5–40 kJ mol^{-1} correspond to physisorption, while values above 40 kJ mol^{-1} denote chemisorption.[176] Positive ΔH indicates endothermic behavior, where elevated temperatures enhance dye diffusion and site activation, while positive ΔS values imply increased disorder at the solid–liquid interface, often linked to desolvation effects during adsorption.

5.3 Process parameters affecting adsorption

Operational parameters significantly influence adsorption efficiency. Solution pH is the most critical factor, as it dictates both the surface charge of the adsorbent and the ionization of dyes.[177] Under acidic conditions, protonated biomass surfaces favor anionic dye adsorption, while alkaline conditions enhance cationic dye uptake *via* electrostatic attraction.[178] Dye removal

Table 4 Adsorption and surface characteristics of magnetized biomass-based adsorbents[a]

Adsorbent	Target dye	q_{max} (mg g^{-1})	K_L (L mg^{-1})	K_f (mg g^{-1}) (L mg^{-1})$^{(1/n)}$	$1/n$	pH_{pzc}	Surface acidity/ basicity (mmol g^{-1})	C : H : N ratio	Ref.
Magnetized rice husk biochar	Methylene blue	210	0.22	42	0.42	6.2	1.35 (acidic)/0.85 (basic)	55.8 : 5.4 : 1.1	164
Fe_3O_4-orange peel composite	Congo red	165	0.18	30	0.55	6.8	1.10/0.92	54.5 : 5.6 : 1.0	165
Magnetized coconut shell biochar	Crystal violet	198	0.3	38	0.39	7.1	1.42/0.88	56.2 : 5.9 : 1.3	166
Fe_3O_4-sugarcane bagasse	Reactive black 5	182	0.26	35	0.48	6.4	1.28/0.90	55.1 : 5.5 : 1.2	167
Magnetized banana peel biochar	Methylene blue	225	0.24	45	0.41	6.6	1.33/0.95	53.8 : 5.8 : 1.0	168
Fe_3O_4-corncob biochar	Malachite green	155	0.15	25	0.6	6.9	1.15/0.84	56.7 : 5.7 : 1.1	169
Fe_3O_4-pine bark composite	Congo red	170	0.2	28	0.52	6.3	1.40/0.91	55.4 : 5.3 : 1.0	170
Fe_3O_4-eucalyptus leaf powder	Basic red 46	160	0.19	32	0.5	6.7	1.26/0.89	54.9 : 5.7 : 1.1	168
Magnetized sawdust biochar	Reactive blue 19	190	0.25	40	0.46	6.5	1.30/0.93	55.2 : 5.4 : 1.2	171
Fe_3O_4-coconut coir composite	Methylene blue	205	0.28	43	0.4	6.8	1.22/0.90	55.7 : 5.5 : 1.1	172

[a] Biomass composition and surface chemistry strongly influence adsorption efficiency. Parameters such as CHN ratio, surface acidity/basicity, and pH_{pzc} provide comparative insight into the adsorbent's functionalization degree and electrostatic behavior.

occurs rapidly within the first 30–60 min due to abundant active sites, then gradually stabilizes as equilibrium is reached.[179] Increasing adsorbent dosage generally improves total dye removal but can reduce adsorption capacity per gram due to particle aggregation and overlapping binding sites.[180]

Temperature affects both diffusion rates and interaction mechanisms. For most magnetized biosorbents, adsorption is endothermic; higher temperatures promote dye mobility and enhance pore diffusion, improving uptake.[181] This trend is supported by reported thermodynamic parameters, where ΔH° values for dye adsorption on magnetized biomass-based sorbents typically range from +10 to +45 kJ mol^{-1}, indicating predominantly physisorption with endothermic character.[182–184]

In addition to pH and temperature, the presence of competing ions in real wastewater systems can markedly influence adsorption performance. Multivalent cations and common inorganic anions may compete with target pollutants for active sites or alter electrostatic and ion-exchange equilibria.[185] Most studies conducted under single-solute laboratory conditions may therefore overestimate removal efficiency. Incorporating competitive ion systems in experimental evaluations provides a more realistic prediction of adsorbent performance under field conditions.

5.4 Mechanistic aspects of dye removal

The efficiency of magnetized biosorbents stems from their combined magnetic separability and surface functional chemistry. Although Fe_3O_4 nanoparticles themselves do not directly adsorb pollutants, they enable rapid recovery of spent adsorbents *via* external magnetic fields, eliminating the need for energy-intensive filtration.[186] These composites can typically be reused for 5–10 cycles with minimal efficiency loss when regenerated using mild desorption agents.[187]

At the molecular level, dye removal is governed by interactions between dye molecules and biomass functional groups—hydroxyl, carboxyl, phenolic, and amine moieties.[188] These groups enable hydrogen bonding, electrostatic attraction, and ion exchange, while aromatic dyes benefit from π–π stacking interactions with lignin-derived structures.[189] The incorporation of magnetic nanoparticles enhances surface area and creates additional active sites, sometimes enabling coordination with dye molecules, further improving removal efficiency.[190] The synergy of these mechanisms enables high adsorption capacities, fast uptake rates, and robust reusability.[191] As depicted in Fig. 3, adsorption efficiency is governed by isotherm models, kinetic behavior, and thermodynamic feasibility, while operational parameters and mechanistic interactions strongly influence overall performance (Fig. 5 and 6).

5.5 Effect of co-existing ions on adsorption performance

Most adsorption studies are conducted using single-component dye systems to establish baseline adsorption behavior. However, in real wastewater, coexisting ions such as Cl^-, SO_4^{2-}, and Ca^{2+} can compete with dye molecules for active sites and influence electrostatic interactions, thereby affecting adsorption efficiency. Several studies have reported that increasing ionic strength can lead to a reduction in adsorption capacity, typically ranging from 15–35%, depending on ion valency, concentration, and surface charge properties of the adsorbent.[192,193] Investigations involving NaCl, $CaCl_2$, and Na_2SO_4 have demonstrated moderate decreases in dye adsorption (approximately 18–27%), confirming that ionic strength and charge competition can

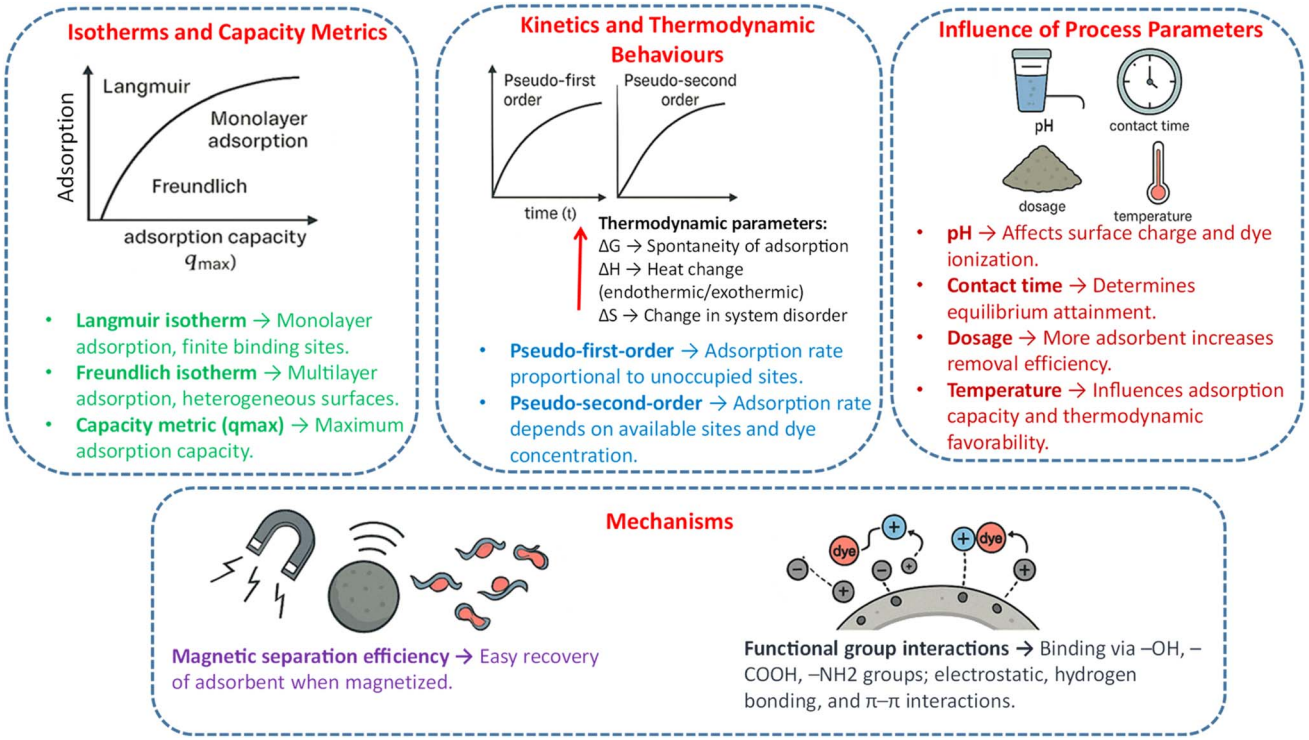

Fig. 5 Adsorption performance metrics and mechanistic insights for dye removal. Isotherm models such as Langmuir and Freundlich describe adsorption behaviour, while kinetic models (pseudo-first- and pseudo-second-order) explain adsorption dynamics. Thermodynamic parameters (ΔG, ΔH, ΔS) indicate spontaneity, heat exchange, and disorder changes. Process efficiency is influenced by pH, contact time, adsorbent dosage, and temperature. Mechanistic pathways include magnetic separation for efficient recovery and functional group interactions with dye molecules.

significantly suppress adsorption performance. These findings underscore the importance of evaluating adsorption in multi-component systems, which more accurately reflect real wastewater conditions. Future research should prioritize systematic studies on the influence of coexisting ions to better understand adsorption mechanisms under practical wastewater

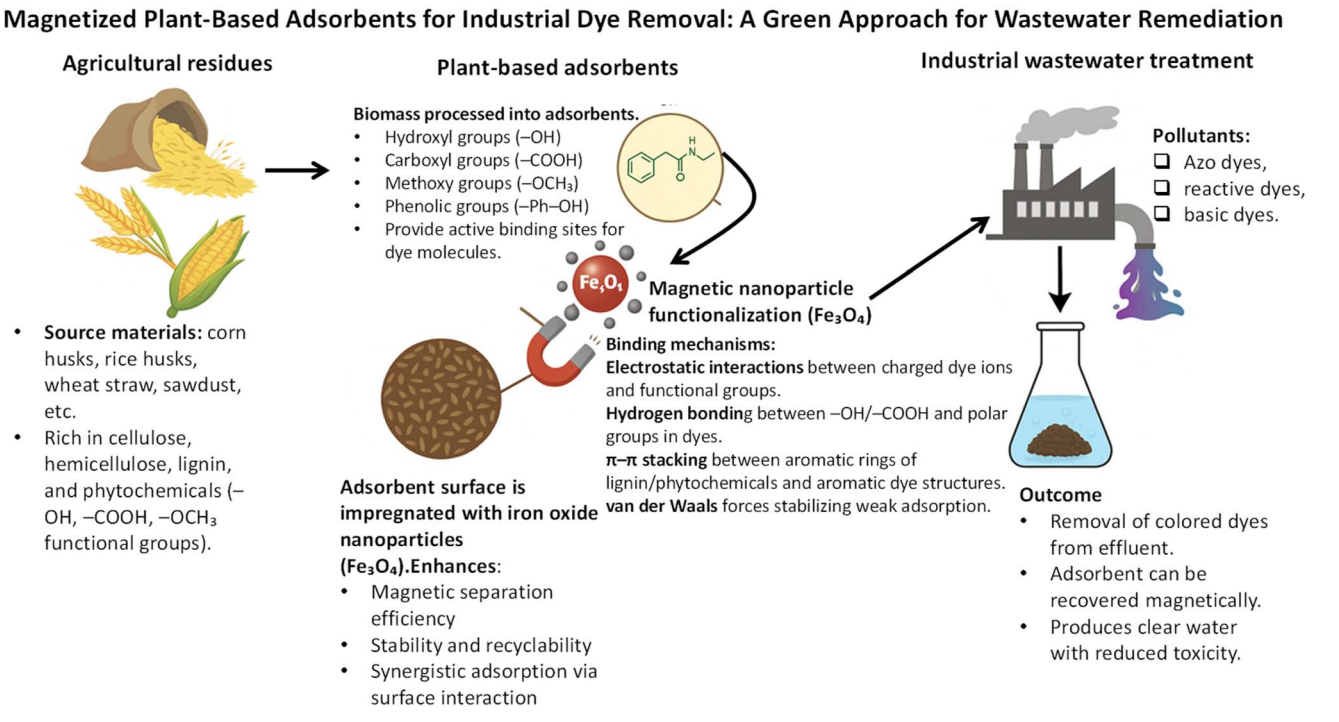

Fig. 6 A schematic overview of magnetized plant-based adsorbents for wastewater remediation.

scenarios and to guide the design of adsorbents with enhanced selectivity and stability in complex matrices.

While most reported studies employ simulated dye-contaminated deionized water, such simplified systems fail to reflect the chemical complexity of natural and industrial wastewaters. Factors such as ionic strength, dissolved organic matter, and colloidal particles can significantly alter adsorption behavior. Future investigations should therefore emphasize validation using real wastewater samples from textile, agrochemical, or pharmaceutical industries to ensure the environmental relevance and scalability of biomass-based adsorbents. Such real-matrix testing would bridge the gap between laboratory results and field performance.

6 Comparative evaluation of magnetized *vs.* non-magnetized plant adsorbents

The modification of plant-based adsorbents with magnetic nanoparticles has demonstrated significant advantages over their unmodified counterparts, not only in enhancing dye removal performance but also in improving operational handling and reusability.

6.1 Improvement in dye removal efficiency

Magnetization typically enhances adsorption efficiency due to increased surface area, improved porosity, and additional active sites provided by Fe_3O_4 nanoparticles.[194] Non-magnetized biosorbents like raw fruit peels or sawdust primarily rely on their inherent cellulose, hemicellulose, and lignin structures for adsorption, which can limit their maximum dye-binding capacity. In contrast, magnetized composites can achieve up to 1.5–2 times higher adsorption capacities, as reported for rice husk and coconut shell biochar magnetized *via in situ* precipitation.[195] Beyond increased capacity, magnetized materials also exhibit faster uptake rates. Nanoparticles contribute to a more accessible pore structure, enhancing intraparticle diffusion.[196] For example, magnetized sugarcane bagasse biochar removed over 90% of methylene blue within 30 min, whereas the non-magnetized form achieved comparable removal only after 90 min.[134]

6.2 Reusability and regeneration potential

One of the most notable advantages of magnetized adsorbents is their ease of recovery and reusability.[197] Non-magnetized biomass typically requires filtration or centrifugation for separation, processes that are time- and energy-intensive and prone to material losses. In contrast, magnetized adsorbents can be efficiently retrieved using external magnetic fields within seconds, simplifying operations and reducing costs.[198] Representative data summarizing the regeneration performance of magnetized biomass adsorbents are provided in Table 5. Across systems including Fe_3O_4-biochar, Fe_3O_4-cellulose, Fe_3O_4-alginate, and Fe_3O_4-chitosan composites, the retained adsorption efficiency after 5–10 cycles typically ranges from 70–90%, depending on the regeneration agent and pollutant type. For instance, magnetized biochar derived from corncob retained 93% of its methyl orange removal capacity after ten regeneration cycles,[199] illustrating the general reusability trend across Fe_3O_4-functionalized biomass adsorbents.

It should be noted, however, that regeneration using acids or salts can alter surface characteristics. Acidic eluents may leach iron ions or protonate functional groups, while salt-based desorption can modify surface charge distribution, influencing subsequent adsorption behavior.[200] Optimization of regeneration conditions is therefore essential to preserve both structural stability and adsorption capacity over multiple cycles. Non-magnetized materials often exhibit greater physical degradation during repeated handling, leading to faster performance decline.[201]

6.3 Long-term stability and iron leaching analysis

The long-term operational stability of magnetic nanoparticles is a critical factor influencing their environmental safety and reusability. Although the current study primarily focused on adsorption efficiency, future investigations should include Fe ion leaching measurements using ICP-OES or AAS to quantify any release of iron during repeated use. Such analyses can

Table 5 Regeneration performance of selected Fe_3O_4-magnetized biomass or carbon-based adsorbents

S. no.	Adsorbent	Pollutant (dye)	Regeneration method	Number of cycles	Retained capacity (%)	Ref.
1	Fe_3O_4/baobab seed-derived biochar (Fe_3O_4/BSB)	Congo red	0.1 M NaOH, wash, reuse	4	80.7% (from ~92.6% after 1st cycle)	202
2	Fe_3O_4-MOS (moringa seed shell biochar)	Methylene blue	Wash + pyro-treatment, reuse	5	~90% retained (removal declined ~9%)	203
3	Fe_3O_4@1 nanocomposite	Methylene blue	Ethanol wash, reuse	7	From ~97.84% → ~90.44% after 7 cycles	204
4	Fe_3O_4–N-banana-peel biomass charcoal	Methylene blue	Not specified	5	High capacity maintained (exact % not detailed)	205
5	Fe_3O_4@granite magnetic adsorbent	Reactive black 5	0.1 M NaOH, reuse	5	49.2% after 5th cycle (from ~85.1% after 1st)	206

confirm the chemical stability of Fe_3O_4 cores and their resistance to oxidation or dissolution under varying pH conditions. Additionally, continuous adsorption–desorption cycling tests should be performed to evaluate the quality loss rate and possible decline in adsorption capacity over multiple cycles.[207] Previous studies have shown that appropriate surface coating (*e.g.*, silica, chitosan, or biochar layers) can significantly minimize Fe leaching (<2% after 10 cycles) and preserve >90% of the adsorption capacity.[208] Incorporating such stabilization strategies would ensure the long-term performance and environmental compatibility of magnetized adsorbents.

6.4 Feasibility in batch and continuous treatment systems

While most research has focused on batch experiments, magnetized plant-based adsorbents are increasingly evaluated in continuous flow systems such as packed-bed and fluidized-bed reactors. Their magnetic properties facilitate real-time recovery and reactivation, reducing clogging and improving system efficiency.[209] In continuous studies, magnetized rice husk composites achieved steady-state dye removal efficiencies exceeding 85% over extended runs, whereas non-magnetized biosorbents suffered from pressure drops and fouling due to particle compaction.[210] Magnetized materials are thus more adaptable for scale-up and integration into industrial treatment trains, particularly where automation and minimal manual intervention are desired.[211] Their stability and separability make them ideal for hybrid systems, combining adsorption with advanced oxidation or biological polishing stages.[212]

7 Real-world applications and case studies

7.1 Treatment of textile and dye manufacturing effluents

Textile industries, responsible for over 60% of global dye discharges, represent the primary target for these adsorbents.[213] Pilot studies using magnetized orange peel biochar and Fe_3O_4-coated rice husk composites have successfully treated real textile effluents containing mixtures of reactive and azo dyes.[214] Removal efficiencies consistently exceeded 85–95% for color and chemical oxygen demand (COD), meeting local discharge standards.[215] These systems demonstrated resilience to variable effluent conditions, including fluctuations in pH, salinity, and organic load.[216] Similarly, magnetized sawdust composites have been employed to treat dye manufacturing waste streams rich in cationic dyes such as crystal violet and methylene blue.[217] Batch and column trials reported sustained removal performance, with effluent color reductions surpassing 90% even after multiple regeneration cycles.[218]

7.2 Pilot-scale demonstrations and scale-up studies

Several pilot-scale studies have validated the scalability of magnetized plant-based adsorbents. In one notable trial, a fluidized-bed reactor employing Fe_3O_4-coated corncob biochar processed 1000 L day^{-1} of textile wastewater for two months, achieving consistent COD reductions of 70–80% and dye decolorization rates of over 90%.[219] The magnetic properties facilitated continuous material recovery and minimized downtime for regeneration, lowering operational costs.[220] Scale-up studies have also highlighted that these adsorbents can be integrated into existing treatment frameworks, functioning as a polishing stage after primary sedimentation or as a replacement for costly granular activated carbon.[221] Their lower production cost and reusability make them competitive, especially in regions where agricultural residues are abundant.[222]

7.3 Economic viability and environmental sustainability

Economic analyses show that magnetized biosorbents can be produced 40–60% cheaper than commercial activated carbon, especially when derived from agro-wastes like banana peels, coconut husks, or rice husks.[223] Although Fe_3O_4 nanoparticle incorporation increases material costs, easy recovery and reusability reduce overall labor and energy expenses.[224] Environmentally, these composites support circular economy goals by valorising agricultural residues and minimizing secondary waste.[225] Their biodegradability ensures that, once spent, they can be safely incinerated or composted, unlike synthetic resins or heavily processed adsorbents.[226] Lifecycle analyses suggest that magnetized biosorbents can reduce the carbon footprint of dye wastewater treatment by over 30% compared to conventional systems.[227]

7.4 Environmental stability and risk mitigation of magnetic nanoparticles

Although Fe_3O_4-based magnetic nanoparticles are widely regarded as biocompatible and environmentally benign, their stability, dissolution, and potential bioaccumulation warrant careful consideration.[228] Under acidic or oxidative conditions, Fe_3O_4 nanoparticles may undergo partial oxidation or leaching, releasing soluble Fe ions that can alter soil and water chemistry.[229] Long-term exposure can also affect microbial communities and enzyme activities, potentially disturbing nutrient cycling.[230] To mitigate these risks, surface modification strategies such as polymer, silica, or carbon coatings have been developed to enhance stability and reduce ion release.[231] Green synthesis approaches further improve environmental compatibility by replacing toxic reagents.[232] Encapsulation within lignocellulosic matrices reduces aggregation and uncontrolled dispersal, providing safer magnetic adsorbents for large-scale use.[233]

8 Challenges and future perspectives

Magnetized plant-based adsorbents hold strong potential for sustainable dye removal, yet challenges related to nanoparticle stability, eco-safe synthesis, and lifecycle impacts remain.[234] Protective coatings enhance stability but increase costs, while green synthesis routes require optimization for scalable and reproducible production. Hybrid materials such as magnetized biochar or MOF-plant composites show promise but face cost and durability barriers. Standardization of adsorption metrics and incorporation of life-cycle and techno-economic assessments are critical for realistic

industrial translation. High-temperature activation and magnetization steps can account for over 60% of total energy inputs, highlighting the need for optimized, low-energy synthesis routes.

9 Conclusion

Magnetized plant-based adsorbents represent more than a sustainable alternative to conventional adsorbents—they signal a paradigm shift toward decentralized, circular, and resource-positive wastewater treatment systems. Their true potential lies in uniting waste valorisation, magnetic recoverability, and low-energy operation within a single remediation platform. Looking ahead, advancing this field requires rethinking material design beyond laboratory-scale metrics, toward functionally adaptive systems capable of operating in complex industrial effluents and varying water chemistries. Integrating multi-functionality, such as catalytic degradation, antimicrobial properties, and selective recognition of dye structures, could transform magnetized phyto-adsorbents from passive sorbents into smart, programmable remediation systems.

To achieve industrial translation, future research must prioritize nano-bio interface stability, safe immobilization of magnetic nanoparticles, minimization of leaching risks, and environmentally responsible end-of-life pathways. The deployment of hybrid architectures—combining biomass-derived carbon frameworks with MOFs, MXenes, or bioenzymatic catalysts—offers promising directions for achieving tunable selectivity and multi-contaminant removal. Equally critical is the integration of techno-economic, LCA, and risk assessment frameworks, enabling realistic evaluation of scalability, social acceptance, and regulatory compliance.

Ultimately, transformative impact of magnetized phyto-adsorbents will rely on collaboration between material scientists, engineers, and industries to transition from conceptual development to pilot-scale demonstration and modular, field-ready reactors. With such advancements, magnetically recoverable plant-based composites could become central to next-generation wastewater treatment infrastructures, supporting global ambitions for energy-efficient, circular, and climate-resilient water purification technologies.

Author contributions

Shaikh Aliya Aijaz: data curation; formal analysis; software; writing – original draft. Zaryab Shafi: conceptualization; software; writing – original draft; writing – review & editing. Mohammad Shahid: resources; writing – review & editing.

Conflicts of interest

The authors declare that they have no known competing financial interests or personal relationships that could have appeared to influence the work reported in this paper.

Data availability

No primary research results, software or code have been included and no new data were generated or analysed as part of this review.

Acknowledgements

The authors SAA and ZA gratefully acknowledge the Department of Applied Chemistry, Faculty of Engineering and Technology, Aligarh Muslim University, Aligarh, and the Department of Biosciences, Integral University, Lucknow, India, respectively, for providing the necessary research facilities.

References

1 T. Islam, M. R. Repon, T. Islam, Z. Sarwar and M. M. Rahman, *Environ. Sci. Pollut. Res.*, 2023, **30**, 9207–9242.
2 H. B. Slama, A. Chenari Bouket, Z. Pourhassan, F. N. Alenezi, A. Silini, H. Cherif-Silini, T. Oszako, L. Luptakova, P. Golińska and L. Belbahri, *Appl. Sci.*, 2021, **11**, 6255.
3 E. O. Alegbe and T. O. Uthman, *Heliyon*, 2024, **10**, 1–19.
4 T. Akter, A. T. Protity, M. Shaha, M. Al Mamun and A. Hashem, in *Nanohybrid Materials for Treatment of Textile Dyes*, Springer Nature Singapore, Singapore, 2023, pp. 401–431.
5 S. Thakur, A. Chandra, V. Kumar and S. Bharti, in *Biotechnology for Environmental Sustainability*, Springer Nature Singapore, Singapore, 2025, pp. 55–100.
6 A. P. Periyasamy, *Sustainability*, 2024, **16**, 495.
7 S. Velusamy, A. Roy, S. Sundaram and T. K. Mallick, *Chem. Rec.*, 2021, **21**, 1570–1610.
8 A. K. Alsukaibi, *Processes*, 2022, **10**, 1968.
9 K. Abhisek, S. S. Vhatkar, H. T. Mathew, P. Singh and R. Oraon, *Discover Chem.*, 2025, **2**, 41.
10 D. S. Rajendran, E. G. Devi, V. S. Subikshaa, P. Sethi, A. Patil, A. Chakraborty, S. Venkataraman and V. V. Kumar, *Clean Technol. Environ. Policy*, 2025, **27**, 649–664.
11 J. Kaur, N. Choudhary and S. Tandon, in *Towards Green Chemical Processes: Strategies and Innovations*, Springer Nature Switzerland, Cham, 2025, pp. 23–49.
12 G. Bal and A. Thakur, *Mater. Today: Proc.*, 2022, **50**, 1575–1579.
13 M. Raninga, A. Mudgal, V. K. Patel, J. Patel and M. K. Sinha, *Mater. Today: Proc.*, 2023, **77**, 286–294.
14 G. Jaria, V. Calisto, V. I. Esteves and M. Otero, *J. Cleaner Prod.*, 2022, **344**, 130984.
15 M. Nasr and M. Samy, in *Sustainable Remediation Technologies for Emerging Pollutants in Aqueous Environment*, Elsevier, 2024, pp. 241–262.
16 S. Dutta, B. Gupta, S. K. Srivastava and A. K. Gupta, *Mater. Adv.*, 2021, **2**, 4497–4531.
17 Y. Aryanfar, H. G. Castellanos, K. A. Hammoodi, M. Farifteh, A. Keçebaş, S. M. Ghasemlou,

A. Mammadova, E. A. Yengejeh and Z. H. Neghabi, *Environ. Prog. Sustainable Energy*, 2024, **43**, e14483.
18 M. Ahmed, M. O. Mavukkandy, A. Giwa, M. Elektorowicz, E. Katsou, O. Khelifi, V. Naddeo and S. W. Hasan, *npj Clean Water*, 2022, **5**, 12.
19 T. Mammburu, Performance of a layered adsorbent column for the removal of chromium and copper using bio-sorbents, PhD Dissertation, University of the Witwatersrand, Johannesburg, South Africa, 2020.
20 A. Rajendran and B. Dhandapani, *Biomass Convers. Biorefin.*, 2025, **15**, 12369–12385.
21 V. Phouthavong, R. Yan, S. Nijpanich, T. Hagio, R. Ichino, L. Kong and L. Li, *Materials*, 2022, **15**, 1053.
22 S. Moosavi, C. W. Lai, S. Gan, G. Zamiri, O. Akbarzadeh Pivehzhani and M. R. Johan, *ACS Omega*, 2020, **5**, 20684–20697.
23 M. Jiang, L. Chen and N. Niu, *J. Mol. Struct.*, 2022, **1260**, 132842.
24 F. S. A. Khan, N. M. Mubarak, Y. H. Tan, R. R. Karri, M. Khalid, R. Walvekar, E. C. Abdullah, S. A. Mazari and S. Nizamuddin, *Environ. Sci. Pollut. Res.*, 2020, **27**, 43526–43541.
25 J. Rammal, A. Daou, D. E. L. Badan, Z. A. Baki, S. Darwich, W. Rammal and A. Hijazi, *J. Chem. Rev.*, 2025, **7**, 566–590.
26 M. Shams, *Polym. Renewable Resour.*, 2024, **15**, 503–516.
27 W. Al-Gethami, M. A. Qamar, M. Shariq, A. N. M. Alaghaz, A. Farhan, A. A. Areshi and M. H. Alnasir, *RSC Adv.*, 2024, **14**, 2804–2834.
28 A. Rajendran and B. Dhandapani, *Biomass Convers. Biorefin.*, 2025, **15**, 12369–12385.
29 L. D. Ardila-Leal, R. A. Poutou-Piñales, A. M. Pedroza-Rodríguez and B. E. Quevedo-Hidalgo, *Molecules*, 2021, **26**, 3813.
30 N. C. Oguanobi, C. O. Aniagor, G. Okoronkwo, C. N. Ude, C. E. Onu and E. N. Anike, in *Engineered Biocomposites for Dye Adsorption*, Elsevier, 2025, pp. 1–10.
31 T. Islam, M. R. Repon, T. Islam, Z. Sarwar and M. M. Rahman, *Environ. Sci. Pollut. Res.*, 2023, **30**, 9207–9242.
32 A. Ayub, A. K. Wani, C. Chopra, D. K. Sharma, O. Amin, A. W. Wani, A. Singh, S. Manzoor and R. Singh, *Bacteria*, 2025, **4**, 15.
33 S. Kasper, O. K. Adeyemo, T. Becker, D. Scarfe and J. Tepper, in *Fundamentals of Aquatic Veterinary Medicine*, Elsevier, 2022.
34 Z. Liao, Y. Zi, C. Zhou, W. Zeng, W. Luo, H. Zeng, M. Xia and Z. Luo, *Int. J. Mol. Sci.*, 2022, **23**, 13148.
35 F. Uddin, *Cellulose*, 2021, **28**, 10715–10739.
36 S. R. Maulik, A. Bhattacharya, P. P. Roy and K. Maiti, in *Textile Dyes and Pigments: A Green Chemistry Approach*, Wiley, 2022, pp. 17–44.
37 M. M. Hassan, J. Harris, J. J. Busfield and E. Bilotti, *Green Chem.*, 2023, **25**, 7441–7469.
38 P. Pandit, K. Singha, S. Maity and S. Ahmed, *Textile Dyes and Pigments: A Green Chemistry Approach*, Wiley, 2022.
39 A. Tariq and A. Mushtaq, *Int. J. Chem. Biochem. Sci.*, 2023, **23**, 121–143.
40 M. Sharma, S. Sharma, M. S. Akhtar, R. Kumar, A. Umar, A. A. M. Alkhanjaf and S. Baskoutas, *Int. J. Environ. Sci. Technol.*, 2024, **21**, 6133–6166.
41 A. P. Periyasamy, *Sustainability*, 2024, **16**, 495.
42 S. S. Affat, *Univ. Thi-Qar J. Sci.*, 2021, **8**, 130–135.
43 H. Alzain, V. Kalimugogo, K. Hussein and M. Karkadan, *Int. J. Res. Rev.*, 2023, **10**, 673–689.
44 O. Edebali, S. Krupcikova, A. Goellner, B. Vrana, M. Muz and L. Melymuk, *Environ. Sci. Technol. Lett.*, 2024, **11**, 397–409.
45 K. T. Chung, *Environ. Sci. Pollut. Res.*, 2016, **23**, 11265–11278.
46 E. Forgacs, T. Cserháti and G. Oros, *Environ. Int.*, 2019, **30**, 953–971.
47 P. Mukherjee, R. S. Sharma and V. Mishra, *Environ. Sci. Pollut. Res.*, 2024, **31**, 1–19.
48 A. S. M. Raja, A. Arputharaj, G. Krishnaprasad, S. Saxena and P. G. Patil, in *Chemical Management in Textiles and Fashion*, Woodhead Publishing, 2021, pp. 79–98.
49 A. M. Jorge, K. K. Athira, M. B. Alves, R. L. Gardas and J. F. Pereira, *Environ. Sci. Technol. Lett.*, 2023, **55**, 104125.
50 A. P. Periyasamy, *Sustainability*, 2024, **16**, 495.
51 X. Muñoz, D. Clofent and M. J. Cruz, *Curr. Opin. Allergy Clin. Immunol.*, 2023, **23**, 70–75.
52 V. S. G. Garcia, L. de Freitas Tallarico, J. M. Rosa, C. F. Suzuki, D. A. Roubicek, E. Nakano and S. I. Borrely, *Environ. Sci. Pollut. Res.*, 2021, **28**, 63202–63214.
53 S. Shabna, C. J. C. Singh, S. D. S. J. Dhas, S. C. Jeyakumar and C. S. Biju, *J. Chem. Technol. Biotechnol.*, 2024, **99**, 1027–1055.
54 R. Christie and A. Abel, *Phys. Sci. Rev.*, 2021, **6**, 557–567.
55 K. Ramamurthy, P. S. Priya, R. Murugan and J. Arockiaraj, *Environ. Sci. Pollut. Res.*, 2024, **31**, 33190–33211.
56 H. Kolya and C. W. Kang, *Toxics*, 2024, **12**, 111.
57 G. K. Zheng, S. K. M. Rozi, Q. Y. Ang, R. Rahamathullah, A. R. W. Yaakub, A. Anuar, F. L. M. Rasdi, M. F. Taha, N. M. Hussein, F. Aburub and S. A. M. Hussin, *Int. J. Environ. Sci. Technol.*, 2025, **22**, 1–17.
58 J. Galloway and D. Lewis, *Environ. Sci. Pollut. Res.*, 2016, **23**, 11265–11278.
59 A. Rodrigues, M. J. Silva and R. Boaventura, *J. Hazard. Mater.*, 2018, **344**, 303–312.
60 A. Massos and A. Turner, *Environ. Pollut.*, 2017, **227**, 194–204.
61 I. F. Neto, P. M. Santos and J. A. Peres, *Chemosphere*, 2019, **223**, 156–164.
62 C. Chen, Z. Yan, Z. Ma, D. Ma, S. Xing, W. Li, J. Yang and Q. Han, *Chin. J. Chem. Eng.*, 2019, **27**, 144–155.
63 J. Li, *Environ. Sci. Pollut. Res.*, 2021, **28**, 4932–4941.
64 S. Sarkar, A. Banerjee and S. K. Mukherjee, *Toxicol Rep*, 2020, **7**, 1280–1289.
65 S. Mishra, R. K. Tripathi and A. Srivastava, *Ecotoxicol. Environ. Saf.*, 2019, **168**, 256–264.
66 R. Patel, N. Shah and M. Desai, *Aquat. Toxicol.*, 2021, **233**, 105763.
67 World Health Organization, in *WHO Guidelines for Drinking-Water Quality*, WHO Press, Geneva, 2020.

68 A. K. Patra and S. R. K. Pariti, *Text. Prog.*, 2022, **54**, 1–101.
69 S. Verma, S. Verma, R. Ramakant, V. Pandey and A. Verma, *Int. J. Hortic. Agric. Food Sci.*, 2025, **9**, 611019.
70 T. Kanjilal and C. Bhattacharjee, in *Organic Pollutants in Wastewater I. Methods of Analysis, Removal and Treatment*, Materials Research Forum LLC, 2018, pp. 1–41.
71 J. Zhao, M. Zhu, W. Jin, J. Zhang, G. Fan, Y. Feng, Z. Li, S. Wang, J. S. Lee, G. Luan and Z. Dong, *J. Nanobiotechnol.*, 2025, **23**, 538.
72 A. Barhoum, J. Jeevanandam, A. Rastogi, P. Samyn, Y. Boluk, A. Dufresne, M. K. Danquah and M. Bechelany, *Nanoscale*, 2020, **12**, 22845–22890.
73 H. Li, X. Chen, D. Shen, F. Wu, R. Pleixats and J. Pan, *Nanoscale*, 2021, **13**, 15998–16016.
74 M. Butnariu and A. I. Flavius, *Biotechnol. Bioprocess Eng.*, 2022, **3**, 1–5.
75 J. Bird, N. Brough, S. Dixon and S. N. Batchelor, *J. Phys. Chem. B*, 2006, **110**, 19557–19561.
76 A. Negi, *Polymers*, 2024, **17**, 36.
77 F. R. Paz-Cedeno, E. G. Solorzano-Chavez, L. M. Dias, C. A. Otaviano, L. J. A. Bustamante, R. Monti, J. P. Martínez-Galán and F. Masarin, in *Hemicellulose Biorefinery: A Sustainable Solution for Value Addition to Bio-Based Products and Bioenergy*, Springer Nature Singapore, Singapore, 2022, pp. 111–137.
78 S. Babel and T. A. Kurniawan, *J. Hazard. Mater.*, 2003, **97**, 219–243.
79 M. Mili, S. A. R. Hashmi, M. Ather, V. Hada, N. Markandeya, S. Kamble, M. Mohapatra, S. K. S. Rathore, A. K. Srivastava and S. Verma, *J. Appl. Polym. Sci.*, 2022, **139**, 51951.
80 Y. Tan, X. Wang, F. Xiong, J. Ding, Y. Qing and Y. Wu, *Ind. Crops Prod.*, 2021, **171**, 113980.
81 I. Chiocchio, M. Mandrone, P. Tomasi, L. Marincich and F. Poli, *Molecules*, 2021, **26**, 495.
82 X. Guan, B. Zhang, Z. Wang, Q. Han, M. An, M. Ueda and Y. Ito, *J. Mater. Chem. B*, 2023, **11**, 4619–4660.
83 Y. Tan, X. Wang, F. Xiong, J. Ding, Y. Qing and Y. Wu, *Ind. Crops Prod.*, 2015, **65**, 342–350.
84 J. A. Okolie, S. Nanda, A. K. Dalai and J. A. Kozinski, *Waste Biomass Valorization*, 2021, **12**, 2145–2169.
85 Y. Sun, J. Cheng, C. Wang and Y. Chen, *Carbohydr. Polym.*, 2019, **207**, 1–10.
86 Q. Zhang, E. Zhu, T. Li, L. Zhang and Z. Wang, *Biomacromolecules*, 2020, **21**, 457–468.
87 A. Hoareau, A. Trindade, M. Jacquet and J. Beaugrand, *Ind. Crops Prod.*, 2018, **122**, 241–251.
88 X. Li, L. Wang and A. Shahbazi, *Biomass Convers. Biorefin.*, 2021, **11**, 2199–2221.
89 Y. Liu, L. Chen, H. Pan and J. Zhang, *Bioresour. Technol.*, 2017, **245**, 1465–1473.
90 C. Chen, Z. Yan, Z. Ma, D. Ma, S. Xing, W. Li, J. Yang and Q. Han, *Chin. J. Chem. Eng.*, 2019, **27**, 144–155.
91 A. Kumar, R. Singh and V. K. Gupta, *J. Environ. Chem. Eng.*, 2020, **8**, 103667.
92 Y. Huang, Z. Liu, J. Liu and H. Wang, *Chemosphere*, 2021, **263**, 128212.
93 M. Umar, S. Zafar, M. Fikry, S. V. Medhe and N. Rungraeng, *Food Rev. Int.*, 2025, **41**, 1–31.
94 H. Gomaa, E. M. Abd El-Monaem, A. S. Eltaweil and A. M. Omer, *Sci. Rep.*, 2022, **12**, 15499.
95 J. D. Faheem, J. Bao, M. A. Hassan, S. Irshad and M. A. Talib, *Arabian J. Sci. Eng.*, 2019, **44**, 10127–10139.
96 Q. Zhang, E. Zhu, T. Li, L. Zhang and Z. Wang, *Biomacromolecules*, 2024, **25**, 6296–6318.
97 S. Yadav, N. Sharma, A. Dalal, P. Panghal, A. K. Sharma and S. Kumar, *Environ. Monit. Assess.*, 2025, **197**, 215.
98 N. Takio, D. Basumatary, M. Yadav and H. S. Yadav, in *Biochemistry: Fundamentals and Bioenergetics*, Bentham Science Publishers, 2021, pp. 55–89.
99 W. Li, Z. Chen, H. Yu, J. Li and S. Liu, *Adv. Mater.*, 2021, **33**, 2000596.
100 J. O. Eniola, B. Sizirici, Y. Fseha, J. F. Shaheen and A. M. Aboulella, *Environ. Sci. Pollut. Res.*, 2023, **30**, 88245–88271.
101 F. M. Jais, *Development of Sugarcane Bagasse-Based Adsorbents for Dye and Antibiotic Removal from Contaminated Water*, PhD thesis, University of Malaya, 2022.
102 K. Harshan, A. P. Rajan, D. Kingsley, R. A. Sheikh, J. Aashmi and A. P. Rajan, *Phys. Sci. Rev.*, 2024, **9**, 1973–1989.
103 N. Gupta, B. K. Mahur, A. M. D. Izrayeel, A. Ahuja and V. K. Rastogi, *Environ. Sci. Pollut. Res.*, 2022, **29**, 73622–73647.
104 A. Albahnasawi, M. Y. Alazaiza, E. Gürbulak and M. Eyvaz, in *Sustainable Nanoremediation*, Apple Academic Press, 2024, pp. 353–389.
105 S. Yaqoob and M. A. Hanif, *Environ. Monit. Assess.*, 2025, **197**, 917.
106 M. T. H. Siddiqui, H. A. Baloch, S. Nizamuddin, N. M. Mubarak, N. Hossain, A. Zavabeti, S. A. Mazari, G. J. Griffin and M. Srinivasan, *Renewable Energy*, 2021, **178**, 587–599.
107 T. Banu, M. Jamal and F. Gulshan, *Results Mater.*, 2023, **19**, 100419.
108 M. M. Ba-Abbad, A. Benamour, D. Ewis, A. W. Mohammad and E. Mahmoudi, *JOM*, 2022, **74**, 3531–3539.
109 M. B. Mahlohla, *Recovery of Fe(III) from Acid Mine Drainage and its Subsequent Application for the Production of Ferric Chloride for Drinking Water Coagulation*, Master's thesis, University of South Africa, 2024.
110 R. Massart, *IEEE Trans. Magn.*, 1981, **17**, 1247–1248.
111 H. Wei, O. T. Bruns, M. G. Kaul, E. C. Hansen, M. Barch, A. Wiśniowska, O. Chen, Y. Chen, N. Li, S. Okada, J. M. Cordero, *et al.*, *Proc. Natl. Acad. Sci. U. S. A*, 2017, **114**, 2325–2330.
112 B. S. Chapman, *Magnetic Functionalization of Silica-Overcoated Gold Nanorods via Heteroaggregation and Direct Electrospinning of Sol Gel Derived Oxide Nanofibers*, PhD thesis, North Carolina State University, 2017.
113 M. M. Khan, in *Photocatalysts: Synthesis and Characterization Methods*, Elsevier, 2025, pp. 11–25.
114 C. Chang, S. Rad, L. Gan, Z. Li, J. Dai and A. Shahab, *Nanotechnol. Rev.*, 2023, **12**, 20230150.

115 L. Lermusiaux, A. Mazel, A. Carretero-Genevrier, C. Sanchez and G. L. Drisko, *Acc. Chem. Res.*, 2022, **55**, 171–185.
116 S. Basak, A. K. Botcha, M. T. Ansari and R. Chandrasekar, *Indian J. Eng. Mater. Sci.*, 2013, **2013**, 136178.
117 M. Wang, J. Shen, X. Xu, H. Feng, D. Huang and Z. Chen, *Sci. Total Environ.*, 2023, **875**, 162652.
118 L. Yang, J. Shen, W. Zhang, W. Wu, Z. Wei, M. Chen, J. Yan, L. Qian, L. Han, J. Li and M. Gu, *Sci. Total Environ.*, 2022, **829**, 154645.
119 R. Wang, Y. Feng, D. Li, K. Li and Y. Yan, *Green Chem.*, 2024, **26**, 9075–9103.
120 Y. Yaqi, C. Ling, Y. Yimin, L. Qi, F. Chengqian, W. Zhiheng, C. Ling, B. Bo, Z. Yue-Fei, L. Yan and W. Li, *J. Mater. Sci.: Mater. Electron.*, 2024, **35**, 215.
121 A. A. Burbano, G. Gascó, F. Horst, V. Lassalle and A. Méndez, *Biomass Bioenergy*, 2023, **172**, 106772.
122 P. Sankaranarayanan, T. A. Anboli and T. V. Suchithra, in *Concepts in Pharmaceutical Biotechnology and Drug Development*, Springer Nature Singapore, Singapore, 2024, pp. 3–20.
123 R. Suhag, R. Kumar, A. Dhiman, A. Sharma, P. K. Prabhakar, K. Gopalakrishnan, R. Kumar and A. Singh, *Crit. Rev. Food Sci. Nutr.*, 2023, **63**, 6757–6776.
124 F. Z. Hamadi, A. O. Ezzat, O. H. Abd-Elkader, A. Benyoucef, B. D. Alkoudsi and L. Sabantina, *Ionics*, 2024, **30**, 4967–4980.
125 M. Sharma, S. Sharma, M. S. Akhtar, R. Kumar, A. Umar, A. A. M. Alkhanjaf and S. Baskoutas, *Int. J. Environ. Sci. Technol.*, 2019, **16**, 6133–6166.
126 R. Rao, S. Patel and V. Deshmukh, *J. Environ. Chem. Eng.*, 2021, **9**, 105432.
127 J. Kumar, P. Kumar and V. K. Chaudhary, in *Int. Conf. Recent Advancements in Mechanical Engineering*, Springer Nature Singapore, Singapore, 2024, pp. 39–55.
128 Y. Li, A. R. Zimmerman, F. He, J. Chen, L. Han, H. Chen, X. Hu and B. Gao, *Sci. Total Environ.*, 2020, **722**, 137972.
129 A. Kumar, A. Kapoor, A. K. Rathoure, G. L. Devnani and D. B. Pal, *Sustain. Proces. Connect*, 2025, **1**, 1–10.
130 L. Yang, J. Shen, W. Zhang, W. Wu, Z. Wei, M. Chen, J. Yan, L. Qian, L. Han, J. Li and M. Gu, *Sci. Total Environ.*, 2022, **829**, 154645.
131 F. Faraji, A. Alizadeh, F. Rashchi and N. Mostoufi, *Rev. Chem. Eng.*, 2022, **38**, 113–148.
132 H. Wei, O. T. Bruns, M. G. Kaul, E. C. Hansen, M. Barch, A. Wiśniowska, O. Chen, Y. Chen, N. Li, S. Okada, J. M. Cordero, *et al.*, *Proc. Natl. Acad. Sci. U. S. A*, 2017, **114**, 2325–2330.
133 J. Li, C. Si, H. Zhao, Q. Meng, B. Chang, M. Li and H. Liu, *Molecules*, 2019, **24**, 3128.
134 L. Yang, J. Shen, W. Zhang, W. Wu, Z. Wei, M. Chen, J. Yan, L. Qian, L. Han, J. Li and M. Gu, *Sci. Total Environ.*, 2022, **829**, 154645.
135 F. M. Jais, *Development of Sugarcane Bagasse-Based Adsorbents for Dye and Antibiotic Removal from Contaminated Water*, PhD thesis, University of Malaya, 2022.
136 M. Sharma, S. Sharma, M. S. Akhtar, R. Kumar, A. Umar, A. A. M. Alkhanjaf and S. Baskoutas, *Int. J. Environ. Sci. Technol.*, 2019, **16**, 6133–6166.
137 R. Rao, S. Patel and V. Deshmukh, *J. Environ. Chem. Eng.*, 2021, **9**, 105432.
138 V. Oriez, J. Peydecastaing and P. Y. Pontalier, *Clean Technol.*, 2020, **2**, 91–115.
139 S. Kaniapan, J. Pasupuleti, K. Patma Nesan, H. N. Abubackar, H. A. Umar, T. L. Oladosu, S. R. Bello and E. R. Rene, *Int. J. Environ. Res. Public Health*, 2022, **19**, 3427.
140 M. Rahman, M. Islam, A. Hossain and M. Hasan, *J. Environ. Chem. Eng.*, 2020, **8**, 103823.
141 E. C. Nnadozie and P. A. Ajibade, *Molecules*, 2020, **25**, 4110.
142 M. A. Mariño, P. Moretti and L. Tasic, *Biomass Convers. Biorefin.*, 2023, **13**, 9265–9275.
143 J. Li, Y. Du, B. Deng, K. Zhu and H. Zhang, *Environ. Sci. Pollut. Res.*, 2016, **23**, 4932–4941.
144 R. Wang, Y. Feng, D. Li, K. Li and Y. Yan, *Green Chem.*, 2024, **26**, 9075–9103.
145 J. Li, Y. Du, B. Deng, K. Zhu and H. Zhang, *Molecules*, 2021, **26**, 3128.
146 P. Jakhar, S. Sharma and H. Sharma, in *Graft Copolymers for Biomedical and Tissue Engineering Applications*, Apple Academic Press, 2025, pp. 219–276.
147 M. A. Akl and A. A. Serage, *Sci. Rep.*, 2024, **14**, 27097.
148 G. Sharma and B. Kandasubramanian, *J. Chem. Eng. Data*, 2020, **65**, 396–418.
149 M. Badoux, M. Billing and H. A. Klok, *Polym. Chem.*, 2019, **10**, 2925–2951.
150 M. A. H. Abdullah, A. H. A. Aziz and N. S. Engliman, *Chem. Nat. Resour. Eng.*, 2024, **8**, 12–27.
151 H. Singh, M. F. Desimone, S. Pandya, S. Jasani, N. George, M. Adnan, A. Aldarhami, A. S. Bazaid and S. A. Alderhami, *Int. J. Nanomed.*, 2023, **18**, 4727–4750.
152 R. T. Kapoor, M. R. Salvadori, M. Rafatullah, M. R. Siddiqui, M. A. Khan and S. A. Alshareef, *Front. Microbiol.*, 2021, **12**, 658294.
153 D. Kirubakaran, J. B. A. Wahid, N. Karmegam, R. Jeevika, L. Sellapillai, M. Rajkumar and K. J. SenthilKumar, *Biomed. Mater. & Devices*, 2025, **1**, 1–26.
154 B. Rezaei, P. Yari, S. M. Sanders, H. Wang, V. K. Chugh, S. Liang, S. Mostufa, K. Xu, J. P. Wang, J. Gómez-Pastora and K. Wu, *Small*, 2024, **20**, 2304848.
155 B. Ates, S. Koytepe, A. Ulu, C. Gurses and V. K. Thakur, *Chem. Rev.*, 2020, **120**, 9304–9362.
156 J. S. Piccin, T. R. S. A. Cadaval Jr, L. A. A. De Pinto and G. L. Dotto, in *Adsorption Processes for Water Treatment and Purification*, Springer, Cham, 2017, pp. 19–51.
157 R. A. Latour, *J. Biomed. Mater. Res., Part A*, 2015, **103**, 949–958.
158 Y. Li, A. R. Zimmerman, F. He, J. Chen, L. Han, H. Chen, X. Hu and B. Gao, *Sci. Total Environ.*, 2020, **722**, 137972.
159 K. C. Ng, M. Burhan, M. W. Shahzad and A. B. Ismail, *Sci. Rep.*, 2017, **7**, 10634.
160 E. Loffredo and E. Taskin, *Environ. Sci. Pollut. Res.*, 2017, **24**, 19159–19166.

161 K. Y. Foo and B. H. Hameed, *Chem. Eng. J.*, 2010, **156**, 2–10.
162 N. Ayawei, A. N. Ebelegi and D. Wankasi, *J. Chem.*, 2017, **2017**, 3039817.
163 A. M. Tawfik and R. M. Eltabey, *J. Phys. Chem. A*, 2024, **128**, 1063–1073.
164 H. Wei, O. T. Bruns, M. G. Kaul, E. C. Hansen, M. Barch, A. Wiśniowska, O. Chen, Y. Chen, N. Li, S. Okada, J. M. Cordero, *et al.*, *Proc. Natl. Acad. Sci. U. S. A*, 2017, **114**, 2325–2330.
165 D. Ghosh, S. Saha and S. Mukherjee, *J. Environ. Chem. Eng.*, 2020, **8**, 104056.
166 Y. Liu, L. Chen, H. Pan and J. Zhang, *Bioresour. Technol.*, 2018, **247**, 687–695.
167 Y. Huang, Z. Liu, J. Liu and H. Wang, *Chemosphere*, 2018, **211**, 404–414.
168 R. Rao, S. Patel and V. Deshmukh, *J. Environ. Chem. Eng.*, 2021, **9**, 105432.
169 Y. Hu, H. Guo, Z. Yu, J. He, Y. Chen and J. Li, *Sci. Total Environ.*, 2019, **646**, 953–963.
170 M. Sharma, S. Sharma, M. S. Akhtar, R. Kumar, A. Umar, A. A. M. Alkhanjaf and S. Baskoutas, *Int. J. Environ. Sci. Technol.*, 2019, **16**, 6133–6166.
171 J. Li, Y. Du, B. Deng, K. Zhu and H. Zhang, *Environ. Sci. Pollut. Res.*, 2016, **23**, 4932–4941.
172 S. Basak, A. K. Botcha, M. T. Ansari and R. Chandrasekar, *Indian J. Eng. Mater. Sci.*, 2013, **2013**, 136178.
173 A. Jatoi, M. Ahmed, S. Khan and A. U. Rehman, *J. Environ. Chem. Eng.*, 2023, **11**, 109245.
174 M. Akbar and S. Ghosh, *Bioresour. Technol.*, 2025, **395**, 130425.
175 J. Kim and Y. Deng, *Chemosphere*, 2023, **318**, 137962.
176 A. Alsharif, *J. Mol. Liq.*, 2025, **403**, 124867.
177 B. Dutta, S. Dutta and P. Mukhopadhyay, *Environ. Sci. Technol. Lett.*, 2021, **40**, 101963.
178 F. Yu, L. Ma, Y. Wang and Z. Li, *Environ. Sci. Pollut. Res.*, 2021, **28**, 28954–28966.
179 R. Mary Ealias and M. Saravanakumar, *J. Environ. Chem. Eng.*, 2019, **7**, 103203.
180 R. Mcyotto, J. O. Mwang'ombe, A. K. Kiprop and E. R. Rene, *Arabian J. Chem.*, 2021, **14**, 103117.
181 E. Güleç, H. Çelebi and E. Şimşek, *Colloids Surf., A*, 2023, **656**, 130423.
182 Y. Li, H. Chen, X. Hu and B. Gao, *Sci. Total Environ.*, 2023, **858**, 159802.
183 B. Dutta, S. Dutta and P. Mukhopadhyay, *Environ. Sci. Technol. Lett.*, 2021, **40**, 101963.
184 F. Yu, L. Ma, Y. Wang and Z. Li, *Environ. Sci. Pollut. Res.*, 2021, **28**, 28954–28966.
185 J. Zhou, X. Wang, Y. Hu and H. Liu, *Water Res.*, 2023, **232**, 119739.
186 S. Fadel, M. El-Sayed, H. Abdelrahman and A. M. Omer, *Sep. Purif. Technol.*, 2025, **330**, 124857.
187 A. El Messaoudi, S. El Ghazouani, R. Taoufik and M. A. Mhamdi, *J. Environ. Manage.*, 2024, **347**, 118912.
188 M. Nizam, S. Ahmad, M. Rafatullah and M. Danish, *J. Hazard. Mater.*, 2021, **416**, 125796.
189 A. Tkachenko, O. Kravchenko and V. Kolesnyk, *Chem. Eng. J.*, 2024, **475**, 146039.
190 A. Moosavi, M. Rahimi and A. Ahmadpour, *Appl. Surf. Sci.*, 2020, **512**, 145722.
191 O. Agboola and N. Benson, *Environ. Technol. Innovation*, 2021, **21**, 101343.
192 R. Wang, Y. Feng, D. Li, K. Li and Y. Yan, *Green Chem.*, 2024, **26**, 9075–9103.
193 Y. Zhang, L. Chen, H. Wang and J. Liu, *Chemosphere*, 2023, **319**, 137987.
194 A. Al-Musawi, S. H. Al-Abbas and M. K. Abbas, *J. Environ. Chem. Eng.*, 2021, **9**, 105480.
195 J. Nie, H. Liu, Y. Zhang, S. Chen and X. Wang, *Bioresour. Technol.*, 2024, **388**, 129684.
196 Z. Wu, J. Chen, Y. Deng, L. Li and J. Wang, *Chem. Eng. J.*, 2020, **395**, 125114.
197 S. Maharana and T. K. Sen, *Environ. Sci. Technol. Lett.*, 2021, **40**, 101915.
198 X. Ren, L. Yang, C. Wang, J. Li and X. Luo, *Sep. Purif. Technol.*, 2021, **276**, 119324.
199 C. Chen, Y. Zhou, J. Li, Q. Zhang and H. Liu, *Sci. Total Environ.*, 2025, **912**, 169058.
200 Y. Liu, Z. He, H. Pan and J. Zhang, *J. Environ. Manage.*, 2023, **336**, 117646.
201 Y. Zhang, M. Ahmed, S. R. Naqvi and B. Gao, *Environ. Res.*, 2024, **241**, 117386.
202 D. A. Daffalla, *J. Environ. Chem. Eng.*, 2025, **13**, 110234.
203 Y. Liu, J. Shen, W. Zhang, W. Wu, Z. Wei, M. Chen, J. Yan, L. Qian, L. Han, J. Li and M. Gu, *Sci. Total Environ.*, 2022, **829**, 154645.
204 J. Li, C. Si, H. Zhao, Q. Meng, B. Chang, M. Li and H. Liu, *Molecules*, 2019, **24**, 3128.
205 Z. Geng, Y. Wang, L. Chen, H. Liu and X. Zhang, *Bioresour. Technol.*, 2024, **388**, 129642.
206 E. Topal Canbaz, *Environ. Technol. Innovation*, 2023, **32**, 103291.
207 A. El Messaoudi, Y. El Khomri, M. A. Khanday, S. Benhadji, M. Barka and A. Assabbane, *J. Environ. Chem. Eng.*, 2024, **12**, 110095.
208 R. Wang, Y. Feng, D. Li, K. Li and Y. Yan, *Green Chem.*, 2023, **25**, 8456–8472.
209 C. Chen and J. Nan, *Chem. Eng. J.*, 2024, **475**, 146658.
210 R. Rao, S. Patel and V. Deshmukh, *J. Environ. Chem. Eng.*, 2021, **9**, 105432.
211 Y. Huo, Z. Liu, J. Wang, S. Chen and X. Zhang, *Water Res.*, 2025, **251**, 120964.
212 O. Lapchuk, A. Malovanyy, M. Nykyforov, M. Kochubei and O. Tymchuk, *Environ. Sci. Technol. Lett.*, 2023, **52**, 103558.
213 S. Periyasamy, *Environ. Res.*, 2024, **241**, 117367.
214 S. Kumar, R. K. Patel and M. A. Shah, *J. Cleaner Prod.*, 2025, **395**, 136507.
215 K. Asaithambi, P. Sivakumar and V. Sivakumar, *J. Environ. Manage.*, 2020, **264**, 110448.
216 J. Salinas-Toledano, A. López-Velázquez, L. E. García-Betancourt and R. Torres, *Water Environ. Res.*, 2025, **97**, e10989.

217 M. Mashkoor and A. Nasar, *J. Environ. Chem. Eng.*, 2020, **8**, 104054.
218 J. Li, X. Zhang, H. Liu and Y. Wang, *Chemosphere*, 2017, **181**, 1–9.
219 Y. Hu, A. R. Zimmerman, X. Gao, H. Chen, L. Han and B. Gao, *Sci. Total Environ.*, 2019, **646**, 532–540.
220 M. Zakeri and A. Tafaghodi, *Process Saf. Environ. Prot.*, 2025, **183**, 154–165.
221 A. Ferri and G. Bolelli, *Sustainability*, 2025, **17**, 2451.
222 M. Blasi, G. Fiorentino, L. Montorsi and G. Manenti, *J. Environ. Manage.*, 2023, **342**, 118086.
223 R. Kiran, P. K. Singh and R. Kumar, *J. Cleaner Prod.*, 2025, **403**, 137040.
224 J. Fuentes, C. Rivera, J. Muñoz and A. Campos, *Resour., Conserv. Recycl.*, 2024, **198**, 107094.
225 J. Jimenez-Lopez, M. Zambrano, R. Torres and E. Rosales, *Bioresour. Technol.*, 2020, **314**, 123735.
226 M. Obodo and O. Agibe, *Environ. Technol. Innovation*, 2023, **31**, 103100.
227 M. Ramadan, H. Abdelrahman and S. El-Sayed, *J. Environ. Chem. Eng.*, 2024, **12**, 109876.
228 S. Hussain, *Ecotoxicol. Environ. Saf.*, 2021, **215**, 112162.
229 A. Dzeranov, A. Kolesnikov, S. Ivanov and E. Frolova, *Environ. Sci. Pollut. Res.*, 2023, **30**, 48621–48634.
230 L. Yang, Z. Liu, Y. Wang and H. Chen, *Appl. Soil Ecol.*, 2021, **168**, 104124.
231 M. Ebrahimi, S. H. Mousavi, R. Behzadfar and A. Fattahi, *J. Hazard. Mater.*, 2025, **456**, 132456.
232 A. Malik, M. N. Siddiqui, R. Khan and S. A. Al-Gaashani, *Green Chem.*, 2023, **25**, 3891–3910.
233 A. Al-Gethami, M. A. Al-Harbi, N. Alshammari and A. A. Al-Farraj, *J. Environ. Chem. Eng.*, 2024, **12**, 109921.
234 Y. Zhao, X. Liu, J. Wang and H. Zhang, *J. Cleaner Prod.*, 2024, **386**, 135781.